

Safety of Automated Driving in Mixed-Traffic Urban Areas

Considering Vulnerable Road Users and Network
Efficiency

Report number: 2020.MME.8472

Author: A.J. Pauwels
Supervisors: Dr. F. Schulte
Dr. N. Pourmohammad-Zia

Table of contents

Acronyms	iv
Preface.....	v
Summary.....	vi
1 Introduction	8
2 Related work	10
2.1 Urban traffic safety	10
2.2 Operational efficiency.....	11
2.3 Occluded sensors.....	12
2.4 Identified gaps.....	13
3 Urban traffic safety assessment	14
3.1 Surrogate safety indicators.....	15
3.1.1 List of symbols	16
3.1.2 Temporal indicators.....	17
3.1.3 Distance-based indicators	22
3.1.4 Deceleration-based indicators	23
3.1.5 Miscellaneous indicators	25
3.2 Swedish TCT.....	26
3.3 Overview of SSI characteristics.....	28
4 Urban traffic efficiency assessment	30
4.1 Macroscopic fundamental diagram	30
4.2 MFD approximation methods.....	31
4.3 Efficiency based on time loss	32
5 Simulation model of the M4H.....	33
5.1 Introduction to SUMO.....	33
5.2 The M4H network.....	35
5.3 The simulated environment	39
5.3.1 Disturbance traffic	39
5.3.2 AV management	39
5.4 Virtual AV model.....	40
5.4.1 Occlusion aware driving principle	40
5.4.2 AV speed controller logic.....	41
5.4.3 SSI devices	48
6 Benchmark of the M4H.....	49
6.1 Safety benchmark	49

6.1.1	Results.....	51
6.2	Efficiency benchmark	54
6.2.1	Results.....	54
6.3	Discussion.....	57
7	Measures and impact on safety and efficiency	59
7.1	Possible measures.....	59
7.2	Safety results	61
7.2.1	Vehicles	61
7.2.2	Pedestrians.....	63
7.3	Efficiency results	64
7.3.1	MFD.....	64
7.3.2	Time loss.....	65
7.4	Discussion.....	68
8	Lessons learned.....	70
9	Conclusion	72
	Bibliography	74
Appendix A	Vehicle parameters.....	79
Appendix B	Additional MFDs (time gap)	81
Appendix C	Additional MFDs (measures)	82

Acronyms

AV	Autonomous Vehicle
ACC	Adaptive Cruise Control
FCFS	First-Come-First-Served
KC	Keep Clear
MFD	Macroscopic Fundamental Diagram
OAD	Occlusion Aware Driving
POMDP	Partial Observable Markov Decision Process
PV	Pseudo Vehicle
SD	Slow Down
SSAM	Surrogate Safety Assessment Model
SSI	Surrogate Safety Indicator
SUMO	Simulation of Urban MObility
V2I	Vehicle to Infrastructure
V2V	Vehicle to Vehicle
V2X	Vehicle to Everything
VRU	Vulnerable Road User

Preface

This Master's thesis is part of the curriculum for the Master of Science in Mechanical Engineering, with the specialization Transport Engineering and Logistics. This research was conducted to contribute to the rapidly evolving topic of autonomous driving. The actual deployment of fully autonomous vehicles without back-up drivers in urban situations has not yet been achieved. My goal was to create a framework in which the interaction between autonomous vehicles, human-driven vehicles, cyclists, and pedestrians in a simulated urban environment could be studied. The effect of various measures on traffic safety and operational efficiency was to be evaluated and recommendations for policymakers were given.

People interested in the traffic safety assessment method should read chapters 3, 6, and 7. Chapters 4, 6, and 7 are for people interested in the operational efficiency assessment methodology. Readers interested in the occlusion aware driving principle and virtual autonomous vehicle model are referred to chapter 5. Chapter 8 presents the lessons learned and some recommendations for policymakers.

Firstly, I would like to thank Dr. Frederik Schulte and Dr. Nadia Pourmohammad-Zia for the opportunity to extend the work of my research assignment to a graduation project. I deeply appreciate their excellent guidance, knowledge, and valuable advice throughout the study. Secondly, I would like to thank the theme coordinator Prof. dr. Rudy Negenborn for the objective evaluation, critical feedback, and being part of the graduation committee.

Delft, 12-1-2021
A.J. Pauwels

Summary

Autonomous vehicles (AVs) are a hot topic today. It is generally accepted that the potential benefits of deploying these vehicles, are an increased road capacity, traffic safety and driving comfort. Companies like Waymo, Tesla, GM Cruise, Baidu, and Argo AI (Granath, 2020) are working on driverless technologies, and some of them are so far in the development that they claim to be safer than humans (Dow, 2019). However, AVs without backup drivers are still far from being deployed in the real world as there are still many technical, safety, legal, and ethical issues surrounding them. To tackle some of these issues, living labs for AVs in urban environments could be created. In these living labs the interaction between autonomous vehicles, infrastructure, conventional vehicles, and pedestrians can be studied. Additionally, there should be room to experiment with different infrastructure, driving behavior, and ways of communication to investigate how these factors influence the safety and operational efficiency of urban traffic networks.

This study investigates the impact of introducing autonomous vehicles in an urban road network on traffic safety and operational efficiency, and how to mitigate the potential impact. The former Merwe- and Vierhavensgebied (M4H) in the Dutch city of Rotterdam was used as a use case. In 2035, this zone should be transformed to a vibrant new part of the city where new manufacturing industry, urban facilities, housing, and culture come together (*Toekomst in de Maak - Ruimtelijk Raamwerk Merwe-Vierhavensgebied Rotterdam*, 2019). It is believed that autonomous freight transport could play a part in the development of new manufacturing industry. The M4H case was used to answer the question: *How could a safe mixed traffic area for autonomous last-mile delivery of cargo be designed while taking operational efficiency into account?*

To identify the research gaps, the literature of the problem was reviewed. It was learned that there are little to no combined urban microscopic simulation frameworks with AVs, human-driven vehicles and Vulnerable Road Users (VRUs) where safety and operational efficiency are assessed. Also, no overview of what influence various measures that can be taken to improve safety and operational efficiency have in urban mixed-traffic (including VRUs) situations is available. Additionally, little AV research in microscopic simulators considers the impact of limited sensorial view caused by obstructions on safety and operational efficiency.

Aside from identifying gaps, the literature review gave insights into traffic safety evaluation and operational efficiency assessment methods. A list of Surrogate Safety Indicators (SSIs) with their characteristics and their calculation procedure was composed, and a selection of SSIs was made to be used in the main experiment. It was learned that efficiency is commonly assessed using Macroscopic Fundamental Diagrams (MFDs) and time loss (delay), which were also taken in our study.

A framework was proposed in which virtual AVs can be injected in the microscopic traffic simulator SUMO and be assessed in terms of safety and operational efficiency. These AVs use an Occlusion Aware Driving (OAD) principle which takes the occluded sensorial view of AVs caused by objects into consideration. At the border of the AV's visibility range, Pseudo Vehicles (PVs) are added. By introducing these imaginary PVs, the AV should never be overwhelmed by a suddenly appearing entity. Although this driving principle is considered perfectly safe, it is also very conservative. To mitigate this conservative behavior, various countermeasures have been investigated by simulating the network in various scenarios.

The safety of a scenario was assessed by first identifying potential accidents using the Swedish TCT (STCT), PET and DRAC with relaxed thresholds. Then the potential accidents were subjected to tighter thresholds for the SSIs: STCT, TTC, TA, TIT, MTTC, CI, PET, PSD, DRAC, CrF and PRI. The number of threshold violations for an SSI was divided by the number of interactions in that scenario. These fractions gave a good approximation of the value of safety slack for the scenarios. MFDs were used to assess the network operational efficiency, and average time loss compared to free-flowing traffic was used to determine the operational efficiency on a vehicular level.

A benchmark was made to verify the safety and operational efficiency assessment model. Several simulation scenarios were created where the desired time gap of the AVs was varied. This variation also affects how fast AVs approach an intersection. The results showed strong evidence that there is a trade-off between safety and efficiency when varying the car-following parameters. It was proven that the safety and efficiency analysis methods are sensitive enough to be influenced by driving parameters.

In the main experiment a total of five additional scenarios with measures were investigated of which three were communication based: V2I, V2V and V2X. The other two were infrastructural based: reducing the maximum allowed speed for some lanes (SD) and keeping a certain area around intersections clear of obstructions (KC). The V2I, V2V, V2X and KC scenarios showed similar levels of safety for trailers, cars, and bikes, but pedestrian safety slightly decreased. The operational efficiency based on time loss of AVs experienced a performance gain of 7.2%, 6.3%, 7.9%, and 3.0% for these scenarios respectively, the time loss of other entities was not affected. Due to the lowered allowed speed in certain lanes, the safety for all entities increased in the SD scenario, but at the cost of lower operational efficiency of all entities.

To answer the main research question: the level of safety is mainly affected by the car-following time gap of the AVs as it adds extra time to execute potential evasive actions, but there is a trade-off between safety and efficiency when varying this parameter. To mitigate conservative behavior of the OAD principle, keeping a certain area around intersections clear could be a design requirement for new buildings as it improves the operational efficiency by 3%. But removing existing objects is not expected to be advantageous as the performance gain of adding any communication device is at least two times larger. Interestingly, the V2I and V2V show only a 0.9% difference in performance gain, favoring V2I. When considering costs, only implementing V2V could be considered as the AVs are already equipped with the correct sensors, but there have to be a certain number of AVs present in the zone to get the desired effect. A benefit of V2I is that they are always present and can collect valuable information of the traffic in zone. The highest performance gain has been achieved by the V2X scenario as it combines V2V and V2I. Other entities show no significant performance gain or reduction in the V2I, V2V, V2X and KC scenarios. In practice, lowering the speed limit is the absolute best way to avoid critical safety situations and reduce the severity of accidents. However, it significantly impacts the delay of all entities, which may provoke dangerous behavior.

1

Introduction

The first attempts of autonomous driving date back to the early 80s and started with the development of on-board vision systems. In 1987, Zapp (1988) successfully demonstrated autonomous driving on a closed part of the German autobahn at speeds up to 96 km/h. It was achieved by using a computer vision system based on control engineering methods and the developing general-purpose microprocessor technology (Dickmanns, 2002). This resulted in the inclusion of this research topic in the EUREKA-project *Prometheus* (Programme for a European traffic of highest efficiency and unprecedented safety). Simultaneously, in the USA the Defence Advanced Research Projects Agency (DARPA) was working on achieving artificial intelligence. One particular research objective was to create computer vision framework based on biological vision systems, which ultimately could be utilized by the guidance systems of autonomous vehicles. Nearly 20 years later, in 2004, DARPA held the first of the three so-called DARPA Grand Challenges where all technologies from the different disciplines of computer science, electrical, robotics and control engineering used in autonomous driving should come together (Urmson et al., 2009). While the first two editions were mainly focused on off-road driving, the third edition in 2007 was centered around urban driving. This is considered a major milestone in the development of autonomous technologies by many researchers. At the time of writing, many companies (Waymo, Tesla, GM Cruise, Baidu, Argo AI, etc.) around the world are working on driverless technology and some already claim to drive safer than humans (Dow, 2019; Granath, 2020). Technical, safety, legal, and ethical issues surrounding autonomous vehicles is holding the mass deployment back.

Autonomous driving in urban environments is significantly harder than driving on motorways as evidenced by the developments in legislation. The transport ministry of the UK announced the allowance of self-driving cars on the UK motorways in 2021 (Topham, 2020). Although they are only allowed to drive in the slow lane and may not overtake, it is a significant step in changing the way cars are driven. For the Netherlands to stay the leader in the autonomous vehicles market of the western world (KPMG, 2020), the need for living labs for autonomous vehicles in urban environments is greater than ever. In these living labs the interaction between autonomous vehicles, infrastructure, conventional vehicles, and pedestrians can be studied. There should be room to experiment with different infrastructure, driving behavior, and ways of communication. This way, guidelines can be created for road construction to future-proof them for the introduction of autonomous vehicles. As of now, not a lot attention is given to this topic.

This research is contributes to the limited knowledge on the impact of introducing AVs in urban networks with respect to traffic safety and operational efficiency for all road users, and how to mitigate the potential impact. The aim of this research is to create a framework similar to the work of Tafidis et al. (2019) in which a simulated scenario with AVs, human-driven vehicles

and Vulnerable Road Users (VRUs) can be assessed on its safety with a large set of Surrogate Safety Indicators (SSIs), and operational efficiency with Macroscopic Fundamental Diagrams (MFDs) and travel time loss. SSIs describe the closeness to or the severity of a collision between two entities in an objective way. In the framework it is possible to experiment with different measures that should increase safety and/or operational efficiency. To ensure safety and realistic behavior of AVs at all times, the AVs in this research take limited sensorial view into consideration with the so-called Occlusion Aware Driving (OAD) principle. The framework will be applied to the former Merwe- and Vierhavensgebied (M4H) in the Dutch city of Rotterdam. In 2035, this zone should be transformed to a vibrant new part of the city where new manufacturing industry, urban facilities, housing, and culture come together (*Toekomst in de Maak - Ruimtelijk Raamwerk Merwe-Vierhavensgebied Rotterdam*, 2019). It is believed that autonomous freight transport could play a part in the development of new manufacturing industry.

In this study the following research question will be answered:

How could a safe mixed traffic area for autonomous last-mile delivery of cargo be designed while taking operational efficiency into account?

The question is divided into five sub questions:

1. How can safety be assessed in urban traffic?
2. How can operational efficiency be measured in urban traffic?
3. What elements should an accurate simulation model of the AV have?
4. How does the network benchmark perform?
5. What measures to increase safety and/or operational efficiency can be taken and what is their impact?

To answer the first two questions a literature review is conducted to investigate the ways of defining safety and operational efficiency of urban road networks. Question three is answered by identifying elements necessary to create an accurate simulation model of autonomous vehicles in an urban road network and a simulation model is created which incorporates these elements. The fourth question is answered by varying the driving model parameters. This results in a benchmark of the zone as of now and verifies the safety and efficiency assessment methods. The last question is answered by creating a list of possible (safety) measures and implementing them in the simulation model. Then, the obtained data from the different scenarios is compared to the previously created benchmark.

The rest of this report is organized as follows: In chapter 2 related work is presented. Chapter 3 lists the identified SSIs, briefly explains the SSIs, and presents the calculation procedures. Urban traffic efficiency assessment methods are presented in chapter 4. The simulation model, including the M4H network and the virtual AV model is presented in chapter 5. In chapter 6, a benchmark is created to get an indication of the default performance on safety and efficiency of the network. In chapter 7, the proposed measures are introduced, implemented, and compared to the benchmark. Chapter 8 is intended for policymakers, and presents the lessons learned from this research. Finally, in chapter 9 conclusions are drawn, limitations are presented, and recommendations for the future research are given.

2

Related work

In this chapter, the literature body of the problem is reviewed., The research mainly fits in with three streams of the literature: urban traffic safety, operational efficiency, and occluded sensors. In the last subsection the identified research gaps are presented.

2.1 Urban traffic safety

In combination with the Surrogate Safety Indicator (SSI) assessment, microsimulation has proven to be a reliable prediction method for collision risk. Mahmud et al. (2017) and Johnsson et al. (2018) did excellent work in reviewing the developments in SSI research and provided an overview of existing SSIs. The work of Johnsson et al. (2018) is especially interesting since it focuses on indicators that are applicable to VRUs. SSI research is limited in this field.

A lot of traffic safety research has already been conducted using SSIs. In the work of G. Guido et al. (2019) historical collision data were found to match with collision data coming from a microscopic simulation which was analyzed using SSIs, in particular the Surrogate Safety Assessment Model (SSAM) of the American Federal Highway Administration. Viridi et al. (2019) used the SSAM to investigate how market penetration of Connected Vehicles (CV) impact safety in a mixed urban and highway situation. They showed that at 90% CV market penetration, the number of conflicts at signalized, priority, roundabout, and diverging diamond intersections are accompanied with a -48%, -100%, -98%, and -81% change, respectively. By analyzing 60 hours' worth of video footage, Essa et al. (2015) calibrated a microscopic simulation model using a genetic algorithm to match the actual behavior of the vehicles. Thirty driving behavior parameters representing the car-following model, lane-change, and signalized intersection parameters were tuned. Using the SSAM, conflict heat maps were generated to compare field-measured with simulated conflict locations. The results highlighted the importance of model calibration and identified several limitations of the SSAM. Li et al. (2016) used the Swedish Traffic Conflict Technique (STCT) to identify and analyze conflicts in video footage. They used the obtained real conflict data and the SSAM tool to successfully calibrate a microscopic traffic simulator. By using the Time-to-Collision (TTC) SSI, they attempted to estimate the Hourly Composite Risk Indexes (HCRI) of the real network with the simulated data by tuning the influencing parameters. The field HCRI and simulation predicted HCRI showed similarities, but were not a perfect match. The STCT in combination with a microscopic simulator was used by Axelsson et al. (2016) to investigate the traffic safety of an intersection in the city center of Stockholm. They compared real world data of two versions of the intersection (old and new) with simulated data to investigate vehicle-pedestrian conflicts. Several issues arose as their real-world data were collected by different observers using different classifications of conflicts. They concluded that with the differences between field observations and simulation evaluation methods in mind, the simulation method can still be

used as an indication for the level of traffic safety. Tafidis et al. (2019) mentioned that existing research is mainly focused on operational efficiency and safety gains of the autonomous vehicle technology without considering Vulnerable Road Users (VRU). In their work the safety (using SSAM) and network performance impact of the introduction of autonomous vehicles and cyclists was studied. They concluded that the average delay and speed in a 0% and 100% market penetration situation are almost the same. However, it was observed that the introduction of AVs in the road network reduced the total number and severity level of cyclist-vehicle conflicts. Another approach to assess traffic safety is taken by Fancello et al. (2019). By using a set of subjective and objective indicators, they performed a multiple-criteria decision analysis (Viktor and Topsis) to rank individual intersections on safety. With this ranking obtained, a plan of priority interventions to improve road safety can be planned. In Table 1, an overview of the related work on safety is presented.

Table 1 Literature table of urban safety assessment studies.

Study	Safety evaluation method			Considered vehicle types				Study area		Data obtained by	
	SSI	AD	MS	AV	CV	BK	PD	UR	HW	SM	RL
Axelsson et al. (2016)	x	x	x	x	x	x	x	x		x	x
Bulla-Cruz et al. (2020)	x	x		x	x			x		x	x
Essa et al. (2015)	x				x			x		x	x
Fancello et al. (2019)		x			x		x	x			x
G. Guido et al. (2019)	x	x			x			x		x	x
Li et al. (2016)	x	x			x			x		x	x
Tafidis et al. (2019)	x		x	x	x	x		x		x	
Virdi et al. (2019)	x		x	x	x			x	x	x	
This research	x		x	x	x	x	x	x		x	

SSI	Surrogate safety indicators	PD	Pedestrians
AD	Actual crash data	UR	Urban
MS	Multiple scenarios	HW	Highway
AV	Autonomous vehicles	SM	Simulation
CV	Conventional vehicles	RL	Real network
BK	Bikes		

2.2 Operational efficiency

In the work of Budan et al. (2018) the impact of introducing connected autonomous vehicles at signalized intersections on operational performance was investigated. They concluded that at low congestion, First-Come-First-served (FCFS) scheduling reduces fuel consumption, average time loss, and queue length with 42%, 96%, and 93%, respectively. At higher congestion states, actuated traffic lights outperform the FCFS scheduling procedure. Wang et al. (2020) researched the effect of autonomous driving in urban environments by representing AVs as vehicles with Adaptive Cruise Control (ACC) and cooperative ACC. The authors generated the Macroscopic Fundamental Diagram (MFD) using a microscopic simulator for 100% manual, 100% ACC, and 100% cooperative ACC driven vehicles in urban environments.

It was concluded that the performance increase in urban environments is significantly lower compared to highway environments. By using an urban grid network with actuated traffic lights, Lu et al. (2018) generated the MFD for six market penetration situations with a mixed fleet of autonomous cars with varying SAE automation levels. The results justified some regularity in the change of the urban MFD. In later research, they also considered a real network alongside the grid network (Lu et al., 2019). This time only SAE level 5 vehicles were considered, and the market penetration was varied. The resulting MFDs from both networks showed that there is a quasi-linear increase in network capacity with increasing market penetration rates. In Table 2, an overview of the related work on operational efficiency is presented.

Table 2 Literature table of simulation based urban efficiency assessment studies.

Study	Efficiency evaluation method			Performance measures				Considered vehicle types				Study area	
	TT	FC	FD	IF	TM	VC	PR	AV	CV	BK	PD	UR	HW
Budan et al. (2018)	x	x		x	x	x		x	x			x	
Lu et al. (2018)	x		x					x	x			x	
Lu et al. (2019)	x		x					x	x			x	
Tafidis et al. (2019)	x							x	x	x		x	
Wang et al. (2020)			x			x	x	x	x			x	
This research	x		x	x		x		x	x	x	x	x	
TT	Travel time loss							AV	Autonomous vehicles				
FC	Fuel consumption							CV	Conventional vehicles				
FD	Fundamental diagram							BK	Bikes				
IF	Infrastructure							PD	Pedestrians				
TM	Traffic management							UR	Urban				
VC	Vehicle communication							HW	Highway				
PR	Prediction												

2.3 Occluded sensors

Autonomous driving is always subjected to uncertainty in occluded regions. Several methods to aid AVs in the decision-process regarding occluded regions have been proposed. Galceran et al. (2015) created an estimation model to track previously unoccluded vehicles in an occluded area. This model was evaluated using a real-world data set obtained from an AV platform. Results showed that this model could estimate the position of an occluded vehicle accurately for a significant amount of time. However, their model relies on the vehicles to be observed before they went into the occluded area, which is often not possible in urban networks. Orzechowski et al. (2018) proposed a safety verification method for vehicle trajectories under occlusions by assuming incoming traffic at the edges of the visibility range and over-estimating their state. This way, safety is always guaranteed as long as evasive maneuvers are possible. A probabilistic approach is proposed by Lee et al. (2017). They used a precise map of an area to predict the motion and to probabilistically model the speed of potential occluded vehicles. With data on these vehicles available, they could calculate the collision risk of trajectories. Yu et al. (2019) extended the work of Orzechowski et al. (2018) and Lee et al. (2017) by researching how these approaches performed at crowded urban intersections. They extended the approach with up to five other vehicles per interaction and showed a significant reduction of collisions and an increase in ride comfort. Lin et al. (2019) used a modified Partial Observable Markov Decision Process (POMDP) in which probabilistic vehicle intentions are considered. The optimal solutions for occluded intersection problems were calculated with a customized POMDP solver, which updated its solutions as soon as new

information was available. This resulted in emulated human-like behavior and was effective in collision avoidance.

2.4 Identified gaps

The review of the literature reveals three main research gaps in the area which are listed as follows:

- There is no combined urban microscopic simulation framework with AVs, human-driven vehicles and VRUs (bikes and pedestrians) where safety and operational efficiency is assessed.
- There is no overview of what influence various measures that can be taken to improve safety and operational efficiency have in urban mixed-traffic (including VRUs) situations.
- Little AV research in microscopic simulators consider the impact of limited sensorial view caused by obstructions on safety and operational efficiency.

These research gaps are filled by proposing a framework in which virtual AVs can be injected in the microscopic traffic simulator SUMO, and be assessed in terms of safety with SSIs and operational efficiency with MFDs and time loss. In the simulated network, trailers, cars, bikes and pedestrians are present. The AVs use an Occlusion Aware Driving (OAD) principle which takes the occluded sensorial view of AVs caused by objects into consideration. At the border of the AV's visibility range, Pseudo Vehicles (PVs) are added which emulate possible occluded vehicles. Although this driving principle is considered perfectly safe in simulated scenarios, it is also very conservative. To mitigate this, the impact of several countermeasures on traffic safety and operational efficiency is to be investigated by simulating the network under various scenarios.

3

Urban traffic safety assessment

Traditionally, road safety is measured by crash rates and the severity of these crashes. Although the approach is well-established, it faces four major concerns. First, the relative infrequency and unpredictability of accidents result in small sample sizes often lacking details regarding failure mechanisms and crash avoidance behavior (Johnsson et al., 2018; Mahmud et al., 2017; Tarko et al., 2009). Second, more severe accidents, especially when insurance payments are involved, are more likely to be reported and small accidents, often involving VRUs are less likely to be reported (Elvik, 1988; Hauer et al., 1988). Similar to the previous concern, near misses and uncomfortable driving situations are expected not to be reported because these encounters are not severe enough. Lastly, ethical problems associated with long-term data collection without taking intermediate actions exist (Mahmud et al., 2017). Especially in the case of accidents involving AVs, it is hard to justify the lack of countermeasures to improve safety.

When talking about traffic safety, it is important to understand the difference between an incident and an accident. An incident is defined as an instance of something happening (event or occurrence). Incidents are not necessarily bad; it just implies that multiple entities have to interact with each other. These interactions in the context of this research may result in actions like slowing down, speeding up, emergency braking and other evasive actions. An accident is an incident which typically results in damage or injury. In the context of this research, an accident is a collision between two entities with a certain severity.

The traditional approach to measure road safety only considers data acquired from accidents. Another approach is the quantitative measurement of safety with the use of Surrogate Safety Indicators (SSIs). In which surrogate implies that incident data are utilized instead of accident data (Johnsson et al., 2018). This method provides relative objective data which is based on closeness to collision of two or more entities. This closeness can be grouped in temporal, distance-based and deceleration-based, there are also some miscellaneous indicators. For surrogate safety indicators to be useful, it is important that there is some kind of relation between the indicators, crash rate, and severity. The process of determining the surrogate safety indicators is often automated with the use of video analysis tools as was demonstrated by Saunier et al. (2007), this allows rich data sets to be collected.

In the following subsection the most-used SSIs are introduced. Thereafter the Swedish TCT is presented. In subsection 3.3, Table 3 an overview of the characteristics of the identified SSIs is given.

3.1 Surrogate safety indicators

The objective of SSIs is to estimate the closeness to and magnitude of damages of a collision. Most indicators estimate crash rate and less estimate severity. There are also some indicators that combine the two. Ideally, there is a linear correlation between the indicator, severity and/or crash rate (Johnsson et al., 2018). It is important to note that there are typically no set thresholds that determine whether a situation is safe or unsafe. When it is not possible to correlate the value of the indicator to an hourly crash rate or crash severity the data becomes more abstract, but can still be an indicator for the safety slack of events.

In this research, only three (crossing, merging, and following) of five possible conflict situations are determined as shown in Figure 1. The other two conflict types are: lane changing, which is similar to merging, and overtaking, which is similar to crossing. These are not specifically covered by any of the indicators presented in this paper, but some indicators can still be applied to these situations. In the next sections the most commonly and some uncommon surrogate safety indicators will be introduced.

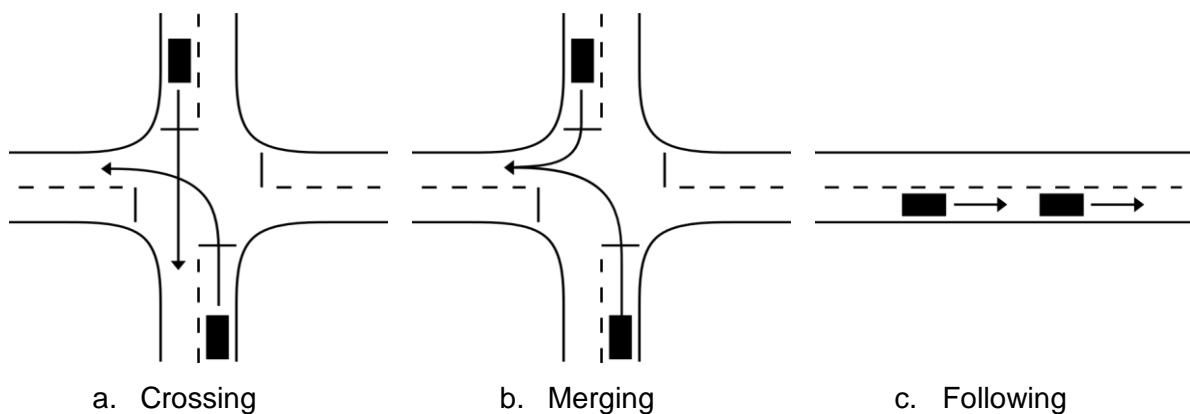


Figure 1 Different conflict situations

3.1.1 List of symbols

Symbol	Definition
t	Point in time [s]
t_a	Time of action [s]
t_c	Time of collision [s]
t_0	Conflict starting time [s]
t_n	Conflict ending time [s]
m_i	Mass of vehicle i [kg]
i	Following vehicle or second vehicle to reach conflict point
j	Leading vehicle or first vehicle to reach conflict point
z	Zebra crossing
c	Collision point
p	Pedestrian
$V_i(t)$	Speed [$\text{m}\cdot\text{s}^{-1}$] of vehicle i
$a_i(t)$	Acceleration [$\text{m}\cdot\text{s}^{-2}$] of vehicle i
$\Delta X_{i,j}(t)$	Bumper-to-bumper distance [m] between entity i and j at time t
$\Delta V_{i,j}(t)$	Relative speed [$\text{m}\cdot\text{s}^{-1}$] between vehicle i and j at time t
$\Delta a_{i,j}(t)$	Relative acceleration [$\text{m}\cdot\text{s}^{-2}$] between vehicle i and j at time t
TTC^*	TTC threshold value [s]
DDS^*	DSS threshold value [m]
τ_{sc}	Small time step [s]
$t_{cp,1}$	Arrival time of conflict point [s]
$t_{cp,2}$	Leaving time of conflict point [s]
t_r	Reaction time [s]
$d_{i,max}$	Maximum deceleration rate of vehicle i [$\text{m}\cdot\text{s}^{-2}$]
α	Impact angle [rad]

3.1.2 Temporal indicators

A total of thirteen 3 temporal SSIs are identified including: Time-to-collisions (TTC), Minimum Time-to-Collision (TTC_{min}), Time-to-Accidents (TA), Time Exposed Time-to-Collisions (TET), Time Integrated Time-to-Collision (TIT), Modified Time-to-Collision (MTTC), Crash Index (CI), Time-to-Zebra (TTZ), Post-Encroachment Time (PET), Encroachment Time (ET), Initially Attempted Post Encroachment Time/Time Advantage (IAPET/TAdv), Conflict Index (Col), Headway/Gap Time (H/GT). Next, these indicators will be briefly addressed.

TTC (Time-to-Collision)

TTC is defined as the time until an accident between two vehicles occurs if they do not alter their trajectory or velocity (Hydén, 1996) and is formulated as equation (3.1). Naturally, the lower the TTC the higher the risk of collision, but it does not give an indication for the severity of the collision. A critical TTC value (TTC^*) can be set as a threshold in order to classify the likelihood of a collision. Generally, this threshold value is the observation and reaction time of the driver and vehicle, while assuming the same deceleration capability. A drawback is that deceleration capability of various vehicle types can differ. Different TTC^* can be set for different conflict situations, from literature was learned that the TTC^* used can wildly vary from 0.9 to 4 seconds (Mahmud et al., 2017). It must be noted that it is possible to have a low TTC while the situation in reality is under excellent control, causing misleading results. This can be the case when connected platooning with a small time gap is deployed.

$$TTC_i(t) = \frac{\Delta X_{i,j}(t)}{\Delta V_{i,j}(t)} \quad 3.1$$

Often all the TTCs in a given time window of a conflict are recorded, depending on the evaluation method, one or more TTCs are chosen for post-processing. This is shown in equation (3.2).

$$TTC_{i,span} = \begin{bmatrix} TTC(t_0) \\ TTC(t_1) \\ \vdots \\ TTC(t_n) \end{bmatrix} \quad 3.2$$

TTC_{min} (Minimum Time-to-Collision)

Since a lower TTC increases the chance of collision, often the TTC_{min} value is subjected to the TTC^* value (equation (3.3)). If the value is lower than the threshold, the incident is reported as critical.

$$TTC_{i,min} = \min(TTC_{i,span}) \quad 3.3$$

TA (Tim- to-Accident)

Another interesting value to subject to the critical TTC value is the TA (equation (3.4)), which is the TTC value at the moment an entity takes action to avoid a collision (Åse Svensson et al., 2006). The advantage of using TA over TTC_{min} is that the safety level at the time an evasive

action is taken is recorded, instead of during or at the end of an evasive action. A disadvantage of TA is that it can be hard to identify the exact moment of the evasive action.

$$TA_i = TTC_i(t_a) \quad 3.4$$

TET (Time Exposed Time-to-Collision)

The TET, calculated with (3.5) and (3.6), is the time an entity spends in a safety-critical situation during an encounter with other entities (Minderhoud et al., 2001). This is represented by the duration the TTC remains below the critical TTC value. A disadvantage of the TET indicator is that it not affected by the amount the TTC is lower than the threshold. Therefore, if the TTC is a little below the threshold value or if it is almost zero, it results in the same TET.

$$TET_i^* = \sum_{t=t_0}^{t_n} \delta_i(t) \cdot \tau_{sc} \quad 3.5$$

$$\delta_i(t) = \begin{cases} 1, & \text{if } 0 \leq TTC_i(t) \leq TTC^*, \\ 0, & \text{else.} \end{cases} \quad 3.6$$

TIT (Time Integrated Time-to-Collision)

To overcome the shortcomings of the TET, Minderhoud et al. (2001) also introduced the TIT indicator. The TIT indicator, computed with equation (3.7), takes the integral of the TTC profile and expresses the level of unsafety in s^2 . As long as the TTC remains below the threshold, the area between the TTC threshold and the TTC is calculated. A visual representation of the TIT and TET factor is presented in Figure 2.

$$TIT_i^* = \sum_{t=t_0}^{t_n} ([TTC^* - TTC_i(t)] \cdot \delta_i(t) \cdot \tau_{sc}) \quad 3.7$$

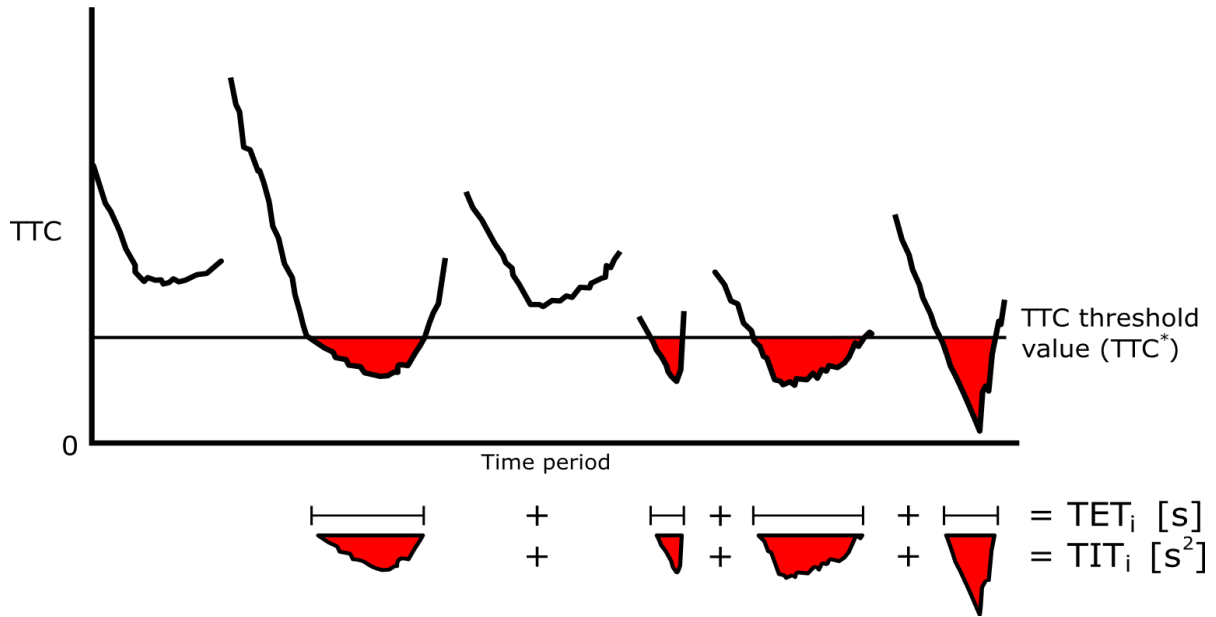


Figure 2 TTC profile with TIT and TET indicated, adapted from Minderhoud et al. (2001).

MTTC (Modified Time-to-Collision)

TTC assumes that both vehicles keep the same speed, and the current acceleration or deceleration is not considered. This neglects the evasive action that is already being taken by the entities. To overcome this shortcoming of TTC, Ozbay et al. (2008) introduced the MTTC. The MTTC takes relative distance, relative speed and relative acceleration into account and better represents the actual time until a collision occurs compared to TTC. MTTC is calculated with equations (3.8) to (3.10).

$$td_{1,i}(t) = \frac{-\Delta V_{i,j}(t) - \sqrt{\Delta V_{i,j}^2(t) + 2 \cdot \Delta a_{i,j}(t) \cdot \Delta X_{i,j}(t)}}{\Delta a_{i,j}(t)} \quad 3.8$$

$$td_{2,i}(t) = \frac{-\Delta V_{i,j}(t) + \sqrt{\Delta V_{i,j}^2(t) + 2 \cdot \Delta a_{i,j}(t) \cdot \Delta X_{i,j}(t)}}{\Delta a_{i,j}(t)} \quad 3.9$$

$$MTTC_i(t) = \begin{cases} \min \begin{pmatrix} td_{1,i}(t) \\ td_{2,i}(t) \end{pmatrix}, & \text{if } td_{1,i}(t) > 0 \text{ and } td_{2,i}(t) > 0 \text{ and } \Delta a_{i,j}(t) \neq 0, \\ td_{1,i}(t), & \text{if } td_{1,i}(t) > 0 \text{ and } td_{2,i}(t) \leq 0 \text{ and } \Delta a_{i,j}(t) \neq 0, \\ td_{2,i}(t), & \text{if } td_{1,i}(t) \leq 0 \text{ and } td_{2,i}(t) > 0 \text{ and } \Delta a_{i,j}(t) \neq 0, \\ TTC_i(t), & \text{else.} \end{cases} \quad 3.10$$

CI (Crash Index)

Since MTTC, like TTC and its counterparts, do not give an indication on the severity of a possible collision, the CI (equation (3.11)) was also proposed by Ozbay et al. (2008). The CI is based on the idea taken from kinetics to consider the effect of speed on kinetic energy at impact. A shortcoming of this approach is that it neglects the mass of the entities as it assumes that different vehicles types do not differ much in mass. This can be misleading when considering conflicts between entities with a big mass difference (e.g. trailer-pedestrian conflict).

$$CI_i(t) = \frac{(V_i(t) + a_i(t) \cdot MTTC_i(t))^2 - (V_j(t) + a_j(t) \cdot MTTC_i(t))^2}{2} \cdot \frac{1}{MTTC_i(t)} \quad 3.11$$

TTZ (Time-to-Zebra)

Várhelyi (1998) introduces a new indicator which is specially adapted for VRUs, in particular pedestrians. The TTZ describes the time until the entity reaches a zebra crossing if it does not change its velocity. It is calculated in the same way as TTC, but neglects the pedestrian's velocity. TTZ is obtained with equation (3.12).

$$TTZ_i(t) = \frac{\Delta X_{i,z}(t)}{V_i(t)} \quad 3.12$$

PET (Post-Encroachment Time)

First introduced by Allen et al. (1978), the PET (equation (3.13)) indicates the time difference between an offending vehicle leaving the conflict area and the arrival time of a vehicle that possesses right of way. The PET therefore represents how close in time the entities were to collision and successfully models the chance of a collision (Alhajyaseen, 2015). PET is considered a robust indicator since it only requires two points in time, and, unlike most TTC-based indicators, does not rely on arrival time estimations.

$$PET_i = t_{cp,2} - t_{cp,1} \quad 3.13$$

ET (Encroachment Time)

Another not so commonly used indicator is the ET; it is defined as the period that a right of way infringing vehicles spends in the conflict zone.

IAPET/TAdv (Initially Attempted Post Encroachment Time/Time Advantage)

IAPET or TAdv are two indicators that are calculated similarly to PET, but it estimate arrival and leaving times of the conflict zone during the conflict instead of calculating PET afterwards (Cooper, 1984; Hansson, 1975). TAdv/IAPET predicts the arrival times based on constant speed and trajectory of both entities (uses TTC).

Col (Conflict Index)

In an effort to estimate the severity of a potential crash using PET, Alhajyaseen (2015) introduced a new indicator that is based on speed, mass, and angle. The Col is similar to CI in that it also uses kinetic energy to express severity, but Col relies on PET instead of MTTC and does take mass and angle of impact into account. The α parameter is the fraction of kinetic energy that affects people inside the vehicles and the β parameter is an adjustment factor for different conflict types. In the original work both parameters were set to 1, but it was stated that the values for these parameters will significantly influence the estimation of the Col. The Col is calculated with equations (3.14) and (3.15), the impact angles θ_x are defined as shown in Figure 3.

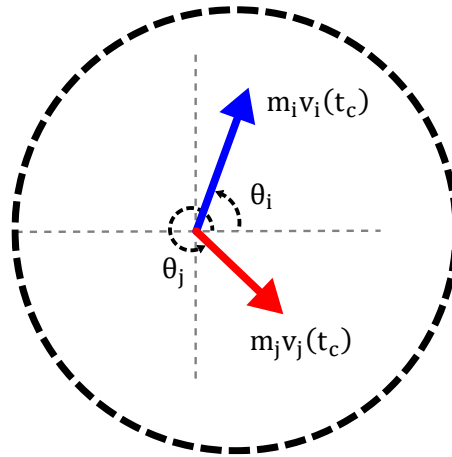


Figure 3 Definition of the impact angles, adapted from Alhajyaseen (2015)

$$Col_i = \frac{\alpha \Delta K_{e_{i,j}}}{e^{\beta PET_i}} \quad 3.14$$

$$\begin{aligned} & \Delta K_{e_{i,j}} \\ &= \left(\frac{m_i v_i^2(t_c) + m_j v_j^2(t_c)}{2} \right) - \frac{1}{2} (m_i + m_j) \\ & \cdot \left(\frac{m_i v_i(t_c) \sin(\theta_i) + m_j v_j(t_c) \sin(\theta_j)}{(m_i + m_j) \sin \left(\tan^{-1} \frac{m_i v_i(t_c) \sin(\theta_i) + m_j v_j(t_c) \sin(\theta_j)}{m_i v_i(t_c) \cos(\theta_i) + m_j v_j(t_c) \cos(\theta_j)} \right)} \right)^2 \end{aligned} \quad 3.15$$

H/GT (Headway/Gap Time)

H/GT is the time gap between two vehicles, it is measured by calculating the time that has passed when two entities have reached the same point.

3.1.3 Distance-based indicators

Five distance-based indicators are identified including: Potential Index for Collision with Urgent Deceleration (PICUD), Proportion of Stopping Distance (PSD), Difference of Space distance and Stopping distance (DSS), Time Integrated Difference of Space distance and Stopping distance (TDSS) and Unsafety (U). These will be introduced in this subsection.

PICUD (Potential Index for Collision with Urgent Deceleration)

PICUD is an indicator used to analyze the crash likelihood for a rear-end collision when the leading vehicle applies its emergency brakes (Uno et al., 2002). It is the distance between two entities when they completely come to a stop, formulated as equation (3.16).

$$PICUD_i(t) = \frac{V_j^2(t) - V_i^2(t)}{2a_{max}} + \Delta X_{i,j}(t) - V_i(t) \cdot t_r \quad 3.16$$

PSD (Proportion of Stopping Distance)

The PSD is defined as the ratio between the remaining stopping distance and minimum stopping distance, equation (3.17) (Allen et al., 1978). If the value is below 1, there is not enough room to stop before reaching the conflict point.

$$PSD_i(t) = \frac{X_{i,c}(t)}{MSD_i(t)} \quad 3.17$$

The acceptable minimum stopping distance (MSD) is calculated using 3.18.

$$MSD_i(t) = \frac{V_i^2(t)}{2 \cdot d_{i,max}} \quad 3.18$$

DSS (Difference of Space distance and Stopping distance)

As introduced by Okamura et al. (2011), DSS (equation (3.19)) in the difference of available space and stopping distance. A value below 0 means the entities will collide. This indicator shares similarity with PSD. The DSS is not an indicator for the severity and does not take duration of conflict into account.

$$DSS_i(t) = \left(\frac{V_j^2(t)}{2d_{j,max}} + \Delta X_{i,j}(t) \right) - \left(V_i(t)t_r + \frac{V_i^2(t)}{2d_{i,max}} \right) \quad 3.19$$

TDSS (Time Integrated Difference of Space distance and Stopping distance)

Okamura et al. (2011) also introduced the TDSS to overcome the shortcoming of DSS. Similar to TIT, the TDSS expresses the level of unsafety in $m \cdot s^{-1}$. Equation (3.20) and (3.21) are adapted from the original research to be able to apply them in discrete time.

$$TDSS_i^* = \sum_{t=t_0}^{t_n} ([DSS^* - DSS_i(t)] \gamma_i(t) \cdot \tau_{sc}) \quad 3.20$$

$$\gamma_i(t) = \begin{cases} 1, & \text{if } 0 \leq DSS_i(t) \leq DSS^*, \\ 0, & \text{else.} \end{cases} \quad 3.21$$

U (Unsafety)

The unsafety indicator developed by Barceló Bugeda et al. (2003). It is only applicable to car-following situations and specially adapted for microscopic traffic simulation. The value does not represent a certain level of safety, it can wildly vary between different types of links. It can, however, be used to assess an increase or decrease in safety of a link. The unsafety is formulated as equation (3.22),

$$unsafety_i(t) = \Delta V_{i,j}(t_c) \cdot V_i(t) \cdot R_{d,j}(t) \quad 3.22$$

$R_{d,j}(t)$ is the ratio between the actual deceleration of the leader over its maximum deceleration, calculated using equation (3.23).

$$R_{d,j}(t) = \frac{-a_j(t)}{d_{j,max}} \quad 3.23$$

3.1.4 Deceleration-based indicators

Four deceleration based indicators were found including: Deceleration Rate to Avoid the Crash (DRAC), Crash Potential Index (CPI), Criticality index Function (CrF) and Deceleration to Safety Time (DST). These will be introduced next.

DRAC (Deceleration Rate to Avoid the Crash)

DRAC was introduced by Almqvist et al. (1991) and considers the impact of differential speed difference in a conflict situation. It is the ratio of the speed differential between leader and follower and their closing time, equation (3.24) (Giuseppe Guido et al., 2012). In urban traffic rapid deceleration is the most common evasive action taken, therefore many researchers recognized that DRAC is one of the most relevant indicators for safety in urban networks (Mahmud et al., 2017). However, many other researchers state that traditional DRAC fails to accurately identify potential conflict because it does not take deceleration capability over time for the current vehicle, road, and traffic conditions into account.

$$DRAC_i(t) = \frac{\Delta V_{i,j}^2(t)}{2 \cdot \Delta X_{i,j}(t)} \quad 3.24$$

CPI (Crash Potential Index)

To mitigate the problems associated with DRAC, F. J. C. Cunto et al. (2007) introduced the CPI. The CPI is the probability that the DRAC exceeds the maximum braking capability of the

entity during its time in the network (F. Cunto, 2008). CPI takes the maximum deceleration of individual links during various conditions into account. The CPI is calculated with (3.25) and (3.26), in the original work the maximum deceleration ($d_{i,max}$) is represented by a truncated normal distribution.

$$CPI_i = \frac{\sum_{t_0}^{t_n} P(d_{i,max} < DRAC_i(t)) \cdot \tau_{sc} b_i(t)}{t_0 - t_n} \quad 3.25$$

$$b_i(t) = \begin{cases} 0, & \text{if no interaction with } j, \\ 1, & \text{if interaction with } j. \end{cases} \quad 3.26$$

CrF (Criticality index Function)

The CrF (equation (3.27)) as proposed by Ching-Yao (2006) is based on two principles. First, the higher the collision speed, the more severe the crash would be. Second, the longer the TTC, the more time to execute an evasive action is available. With these two principles in mind, he defined the CrF as the squared speed of the oncoming vehicle divided by the TTC. It is believed to be a meaningful index to assess severity of a collision, but lacks further evaluations (Mahmud et al., 2017).

$$CrF_i(t) = \frac{V_i^2(t)}{TTC_i(t)} \quad 3.27$$

DST (Deceleration to Safety Time)

First introduced by Hupfer (1997), the DST describes the minimum required deceleration to turn a possible collision situation into a near miss situation. DST does not take current deceleration rate into account and can only be used to assess collision risk, not severity. It is designed to be applied on pedestrian-vehicle conflicts, but can also be applied on vehicle-vehicle conflicts. DST is calculated using equation (3.28).

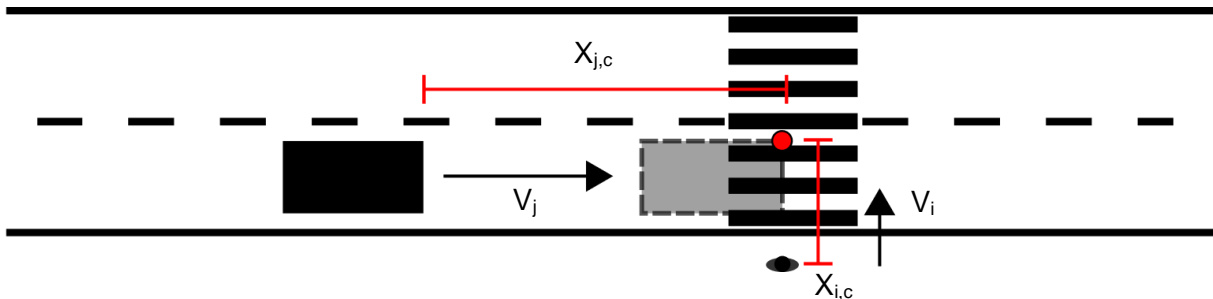


Figure 4 Values to calculate DST, adapted from Hupfer (1997)

$$DST_i(t) = \frac{2 \left(X_{j,c}(t) - V_j(t) \cdot TTC_i(t) \right)}{TTC_i^2(t)} \quad 3.28$$

3.1.5 Miscellaneous indicators

Three miscellaneous indicators remain: DeltaV, Conflict Severity (CS) and Pedestrian Risk Index (PRI).

DeltaV

DeltaV is defined as the change in velocity between pre- and post-collision trajectories of a vehicle, it gives an indication for the severity of a collision (Shelby, 2011). It is considered to be the best single predictor of crash severity by some researchers. DeltaV assumes that momentum is conserved during an inelastic collision between two vehicles. The two dimensional DeltaV is calculated using equation (3.29) (Bagdadi, 2013).

$$DeltaV_i = \frac{m_j}{m_i + m_j} (V_j(t_c) + V_i(t_c) \cdot \cos(\alpha)) \quad 3.29$$

CS (Conflict Severity)

CS is a combination of DeltaV, TA and maximum deceleration as formulated in equation (3.30). It is a combined factor which captures crash risk and severity and is applicable for all conflict types (Johnsson et al., 2018). Because CS also considers mass, deceleration rate and impact angle of the vehicles, it estimates the dangerousness of all conflict types in a more realistic manner than the classical TA. (Bagdadi, 2013)

$$CS_i = DeltaV_i - \frac{m_j}{m_i + m_j} (TA_i \cdot d_{i,max}) \quad 3.30$$

PRI (Pedestrian Risk Index)

The PRI is a measure for crash potential and severity on zebra crossings as introduced by Cafiso et al. (2011). PRI combines the TTZ with assumptions about reaction time and deceleration capability (Johnsson et al., 2018). The collision risk is defined by the difference in stopping time and TTZ and the severity by the squared impact speed. The calculations for the PRI has been adapted from Cafiso et al. (2011) to be homogenous with the rest of this paper. The stopping time of the approaching vehicle is calculated with (3.31).

$$t_{i,stop}(t) = t_r + \frac{V_i(t)}{d_{i,max}} \quad 3.31$$

Collision risk is estimated with equation (3.32).

$$\Delta T_i(t) = t_{i,stop}(t) - TTZ_i(t) \quad 3.32$$

The impact speed (severity) is calculated with equation (3.33) and takes reaction time and current deceleration into account.

$$V_{impact}(t) = \sqrt{V_i(t)^2 - 2a_i(t) \cdot (X_{i,z}(t) - V_i(t) \cdot t_r)} \quad 3.33$$

To determine whether the pedestrian is in conflict with the vehicle, equation (3.34) is used.

$$\kappa_i(t) = \begin{cases} 1, & \text{if } TTC_p(t) < TTC_i(t) < t_{i,stop}(t), \\ 0, & \text{else.} \end{cases} \quad 3.34$$

Finally, the PRI (equation (3.35)) is calculated by taking the sum of the squared impact speed times the difference between stopping time and TTZ with adjustments for simulation step size.

$$PRI_i = \sum_{t=t_0}^{t_n} \left((V_{impact}^2(t) \cdot \Delta T_i(t)) \kappa_i(t) \cdot \tau_{sc} \right) \quad 3.35$$

3.2 Swedish TCT

The Swedish Traffic Conflict Technique (TCT) was developed in the 1970s by the University of Lund. It is one of the oldest, well-tested and well-validated TCT, still being used by road safety assessors today (Laureshyn et al., 2018). The method can be used to identify and classify traffic conflicts based on TA and Conflicting Speed (CS), which is the speed of the vehicle when it takes an evasive action. As roads were becoming safer in the early 1990s, longer observation periods were required to obtain a sufficient amount of data. Therefore, the use of the technique became less frequent as most of these observations were done by humans. Then, with introduction of video and simulation tools, that can record and analyze these conflicts automatically, interest in the technique was revived. The Swedish TCT (STCT) is still being modified as the latest revision is from 2018. Although the method has been altered many times over its existence, the basics remained the same:

- The requirement for a collision course in a conflict;
- The definition of conflict severity based on the onset of an evasive action;
- The distinction between serious and non-serious conflicts. The serious conflicts were found to be an indicator of a breakdown in the interaction – similar to a breakdown preceding an accident.

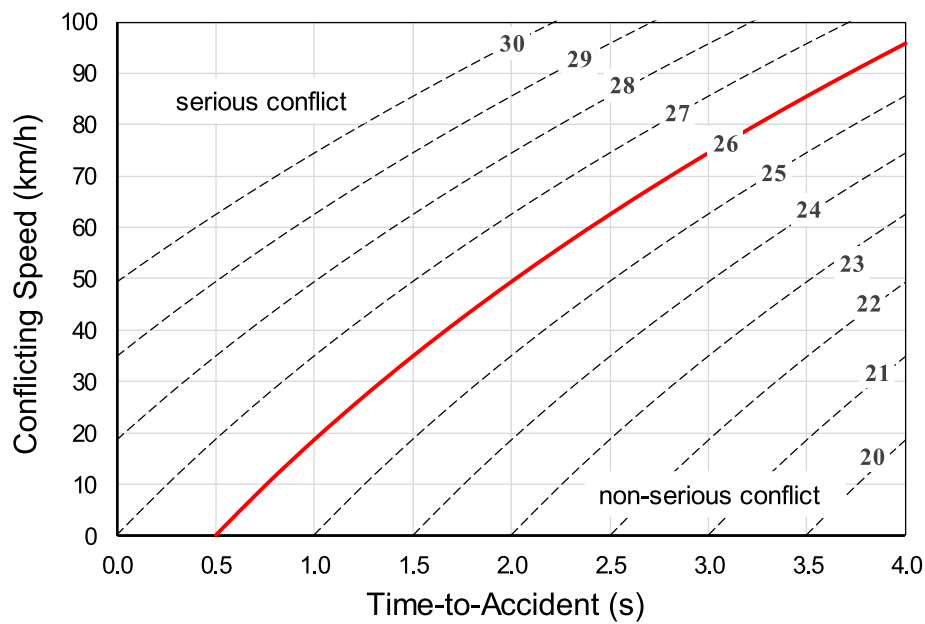


Figure 5 TA/CS graph with the severity levels as defined by the Swedish TCT indicated, adapted from Laureshyn et al. (2018)

Figure 5 shows the relation between seriousness, CS and TA. This graph is used to determine the level of seriousness of an incident. If TA increases, the seriousness decreases as there is more time to execute the evasive action. If the CS increases, the required time to execute an evasive action increases and thereby the seriousness increases. When the level of severity is above 26, the conflict is considered serious (Laureshyn et al., 2017). There is a strong statistical relation between police-reported accidents and serious conflicts (Å Svensson, 1992). It is possible to convert these serious conflicts to an expected number of accidents with reasonable accuracy, even if these accidents happen rarely.

The STCT can be applied to conflicts of the vehicle-vehicle (including bikes) type and vehicle-pedestrian type as long as the pedestrian is not taking the evasive action (Axelsson et al., 2016). Pedestrians can quickly stop or jump, and doing so makes it hard to determine how close the situation to an actual collision was.

Due to its simplicity and objectivity the Swedish TCT is the most well-known TCT, but several alternative techniques from other countries do exist: the Austrian (Risser et al., 1991), Canadian (El-Basyouny et al., 2013), Czech (Kočárková, 2012), Dutch (Kraay et al., 2013), Finnish (Kulmala, 1984), French (Muhlrad et al., 1984), German (Erke et al., 1985), British (Baguley, 1984) and American (Parker Jr et al., 1989) TCT. These are well documented in literature, addressing those individually is out of the scope of this research.

3.3 Overview of SSI characteristics

Table 3 The identified SSIs and their characteristics.

SSI	Conflict type			Indicator type		Span or one value									Interaction		Used in this research	
	Car-following	Merging	Crossing	Crash risk	Severity	Span maximise	Span minimise	One value	Distance	Speed	Acceleration	Mass	Conflict angle	Reaction time	Conflict duration	Vehicle-vehicle		Vehicle-pedestrian
TTC	x	x	x	x			x		x	x						x	x	x
TA	x	x	x	x				x	x	x						x	x	x
TET	x	x	x	x				x	x						x	x	x	
TIT	x	x	x	x				x	x						x	x	x	x
MTTC	x	x	x	x			x		x	x	x					x	x	x
CI	x				x	x			x	x	x					x		x
TTZ			x	x			x		x	x							x	x
PET		x	x	x				x								x	x	x
Col	x	x	x		x			x		x		x	x			x	x	
H/GT	x			x			x									x		
PICUD	x			x		x			x	x	x			x		x		
PSD	x	x	x	x			x		x	x	x					x	x	x
DSS	x			x		x			x	x	x					x		
TDSS	x			x				x	x	x					x	x		
U	x			x		x				x	x					x		

SSI	Conflict type			Indicator type		Span or one value									Interaction		Used in this research	
	Car-following	Merging	Crossing	Crash risk	Severity	Span maximise	Span minimise	One value	Distance	Speed	Acceleration	Mass	Conflict angle	Reaction time	Conflict duration	Vehicle-vehicle		Vehicle-pedestrian
DRAC	x	x	x	x		x			x	x						x	x	x
CPI	x	x	x	x				x	x	x						x	x	
CrF	x	x	x		x	x			x	x						x	x	x
DST	x	x	x	x		x			x	x						x	x	
DeltaV	x	x	x		x			x	x			x	x			x	x	
CS	x	x	x	x	x			x	x	x		x	x			x	x	
PRI			x	x	x			x	x	x				x	x		x	x
STCT	x	x	x	x	x			x	x							x	x	x

4

Urban traffic efficiency assessment

This chapter is dedicated to urban traffic safety assessment. First, Macroscopic Fundamental Diagrams (MFDs) are introduced, and how to obtain MFDs is addressed. In the last subsection, efficiency assessment based on time loss is introduced and several concerns are mentioned.

4.1 Macroscopic fundamental diagram

The MFD was first described by Greenshields et al. (1935). They investigated the relation between traffic density and flow by analyzing a single unsignalized street in the state of Ohio. In the 1960s this idea was extended to complex urban networks (Godfrey, 1969; Payne, 1979; Smeed, 1968) and the relationship between traffic density, flow and speed was investigated. The first convincing empirical evidence of the existence of urban MFD was found by Daganzo et al. (2008). Later, several other studies with real world data were carried out in the networks of Shanghai and Rome (Zhang et al., 2020) confirming its existence.

MFDs are widely used as a tool in the design process of highway road networks, but they can also be used to describe the aforementioned relation in urban networks. A typical MFD consists of a set of three plots: *density-flow*, *density-speed*, and *speed-flow*. All plots are related to the fundamental relationship given in equation 4.1 where Q denotes the flow [$vehicles \cdot h^{-1}$], V the average speed [$km \cdot h^{-1}$] and ρ the vehicle density [$vehicles \cdot km^{-1}$]. In Figure 6 an example of a typical MFD is given.

$$Q = V \cdot \rho \tag{4.1}$$

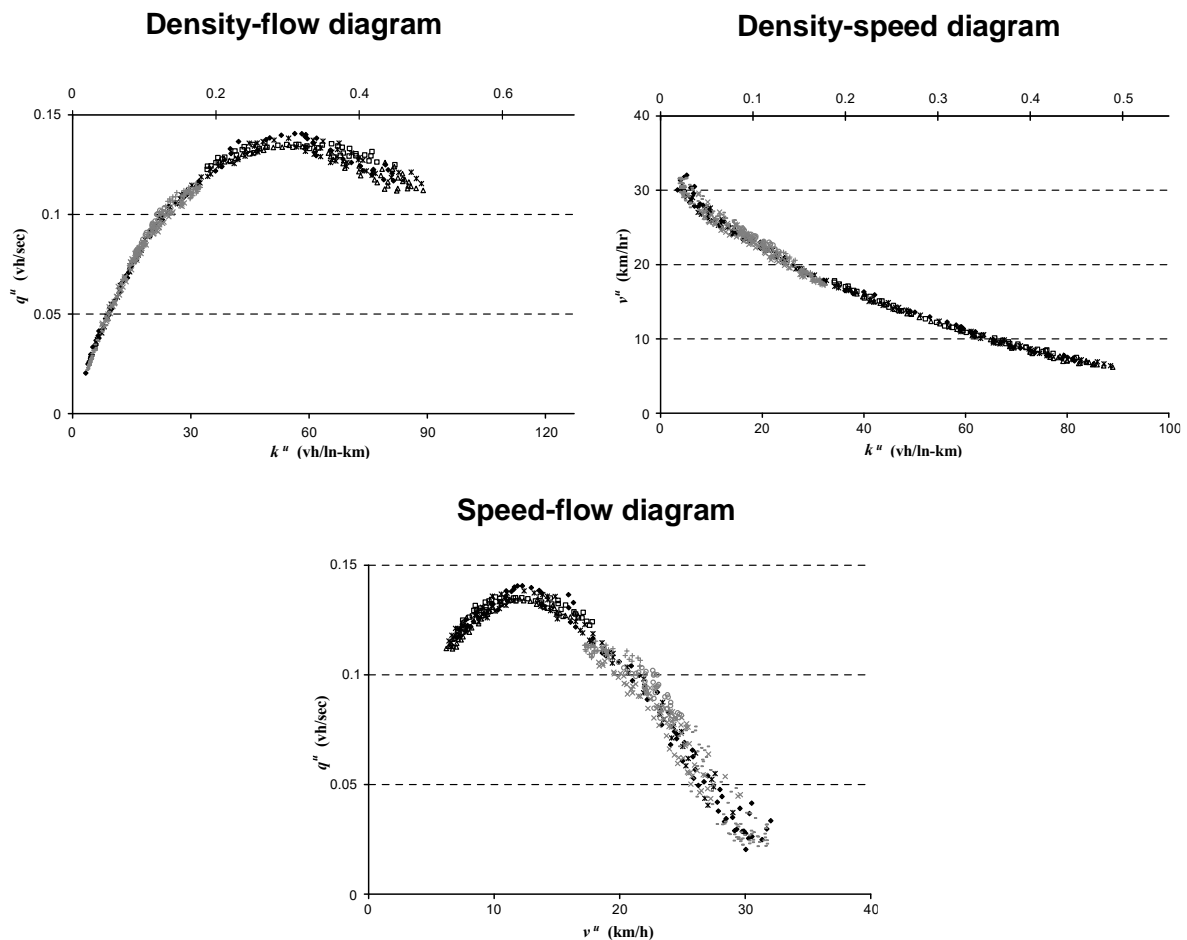


Figure 6 Typical MFD, adapted from Helbing (2009).

4.2 MFD approximation methods

There are two ways to obtain the MFD from a road network: the analytical derivation and experimental analysis from real or simulated data (Zhang et al., 2020). Among the analytical models, the most studied variant is based on variational theory (Daganzo, 2005) and practical cuts (Daganzo et al., 2008). These models are limited to homogenous (grid) networks and signalized intersections. Its application got extended with parallel roads and weak heterogeneity in the studies of Geroliminis et al. (2012) and Leclercq et al. (2013). However, they did not entirely overcome the earlier mentioned limitations. Another analytical approach for approximating the MFD is by linear programming as demonstrated by Daganzo et al. (2016). This model not only allows for the derivation of the MFD, but can also be used to optimize traffic signals lengths at intersections. The stochastic model as proposed by Laval et al. (2015) is based on variation theory and the cuts method. This model was verified with exact traffic data of the city of Yokohama, Japan. Furthermore, Helbing (2009) derived an analytical model to predict MFDs based on expected traffic flows on intersections. The average travel time and average vehicle speed can be expressed in terms of network utilization and/or the average number of delayed vehicles.

Collecting good quality real-world data of traffic in an entire network is notoriously hard. There are several ways to collect real-world data, some examples are: the use of loop detectors, probe vehicles, camera footage and most recently Bluetooth/Wi-Fi/cellular sniffers (Gayah et al., 2013; Geroliminis et al., 2008; Leclercq et al., 2014; Shoufeng et al., 2013). This kind of

data are often combined with analytical data to fill in measurement gaps to ultimately get an estimation for the MFD of the entire network.

4.3 Efficiency based on time loss

From the related work section one can learn that aside from MFDs, time loss (or delay) is often used as a measure of efficiency. Where MFDs describe the performance on the network level over the entire congestion spectrum, time loss describes the performance on a vehicular level at a particular level of service. A benefit of using time loss is that it is easier to understand, and can be calculated per vehicle type. While MFDs are rather abstract, and always consider all entities in (a part of) the network or on a lane. When using time loss as an indicator for operational performance, it is essential to constantly have the same level of service (for instance the same number of running vehicles) in these comparison cases.

5

Simulation model of the M4H

The former Merwe- and Vierhavensgebied (M4H) in the Dutch city of Rotterdam will be the use case in this research. This area has always been part of the port of Rotterdam, but as the industry grew over the years most of the port activities moved to the Maasvlakte area. This area has more physical space, can accommodate larger ships, is closer to the sea and has a better connection to the arterial (railway and road) networks of Europe. As the industry moved more and more from the city to the Maasvlakte, the port and city got separated. This left the municipality with large, partly unused areas close to the city center. To put these areas back into use and reconnect the port to the city, Rotterdam started the M4H project. The aim of the project is to repurpose the former port area by joining the so-called Makers District, which the former RDM area pioneered (*Toekomst in de Maak - Ruimtelijk Raamwerk Merwe-Vierhavensgebied Rotterdam*, 2019). The Makers District consists of several sub-areas which all have a different mixture of new manufacturing industry, urban facilities, housing, and culture. These areas have to serve as an innovation environment for new manufacturing industry made possible by digitization and robotization without harming people and the environment. To accommodate this new industry the proximity of creative talent, the market and knowledge centers are essential.

The spatial framework provided by the M4H team offers a glance into the future of M4H. The framework offers a map of the M4H in 2035 and a look ahead to 2050. The provided map serves as the basis of the use case. In the framework, an autonomous vehicle route is suggested which is specially designed for autonomous public transport. As autonomous freight transport will undoubtedly play a part in the development of new manufacturing industry, the idea is to extend the suggested route to support such autonomous transport. To investigate what infrastructure, driving behavior and communication systems are essential for safe and efficient transport, this research is conducted. Using the microscopic traffic simulator SUMO (*Simulation of Urban MObility*), the network as proposed in 2035 and the introduction of AVs will be subjected to safety and operational efficiency assessment.

5.1 Introduction to SUMO

The opensource microscopic traffic simulation package SUMO (*Simulation of Urban MObility*) is used to create a digital representation of the M4H zone in Rotterdam to study the impact of AVs with limited sensor range. SUMO was developed by the German Aerospace Center and its community members. It has been freely available since 2001.

Traffic simulators can be grouped into three classes: macroscopic, microscopic and mesoscopic (Siegel et al., 2005). Macroscopic simulators represent traffic as an average

vehicle flow between links in a network. When simulating on a microscopic level all vehicles are considered as entities and behave in their own way, this comes at the cost of simulation speed. Lastly, mesoscopic simulation is combination of macroscopic and microscopic, where groups of vehicles are considered an entity and are modelled like a flow on links. As mentioned earlier, SUMO falls in the microscopic category. It is lightweight and therefore capable of simulating large complex networks on a microscopic level.

Aside from the main simulation program, the SUMO suite is packed with useful tools such as *netconvert*, *Duarouter* and *TraCI*. *Netconvert* and *NetEdit* are the tools to convert various network formats to the SUMO format and edit networks. There is also the possibility to build traffic networks from OpenStreetMaps with the *OSM Web Wizard tool*. *Duarouter* is used to generate vehicle routes. It generates the shortest path from A to B via C. The last useful tool is *TraCI*. It is short for Traffic Control Interface and allows for on-line manipulation of the simulation, meaning it can retrieve and set variables. There is a python API available for *TraCI* which is used in this study.

A network in SUMO consists of nodes and links between nodes. The nodes represent junctions, and the links are called edges. An edge can consist of one or more lanes, are always unidirectional and have a priority value. Various lane types are defined in SUMO: unrestricted lanes (all traffic is allowed) and restricted lanes (bike lanes, sidewalks, or any other vehicle exclusive lanes). For each lane, the width and maximum speed can be set. A junction in SUMO consists of connections between lanes and pedestrian crossings. There are two types of pedestrian crossings: unprioritized and prioritized. From now on, prioritized crossings will be referred to as zebra crossings. In Figure 7, one junction is shown with labeled key components. From this figure one can see that a junction quickly becomes complex even if there are a moderate number of lanes.

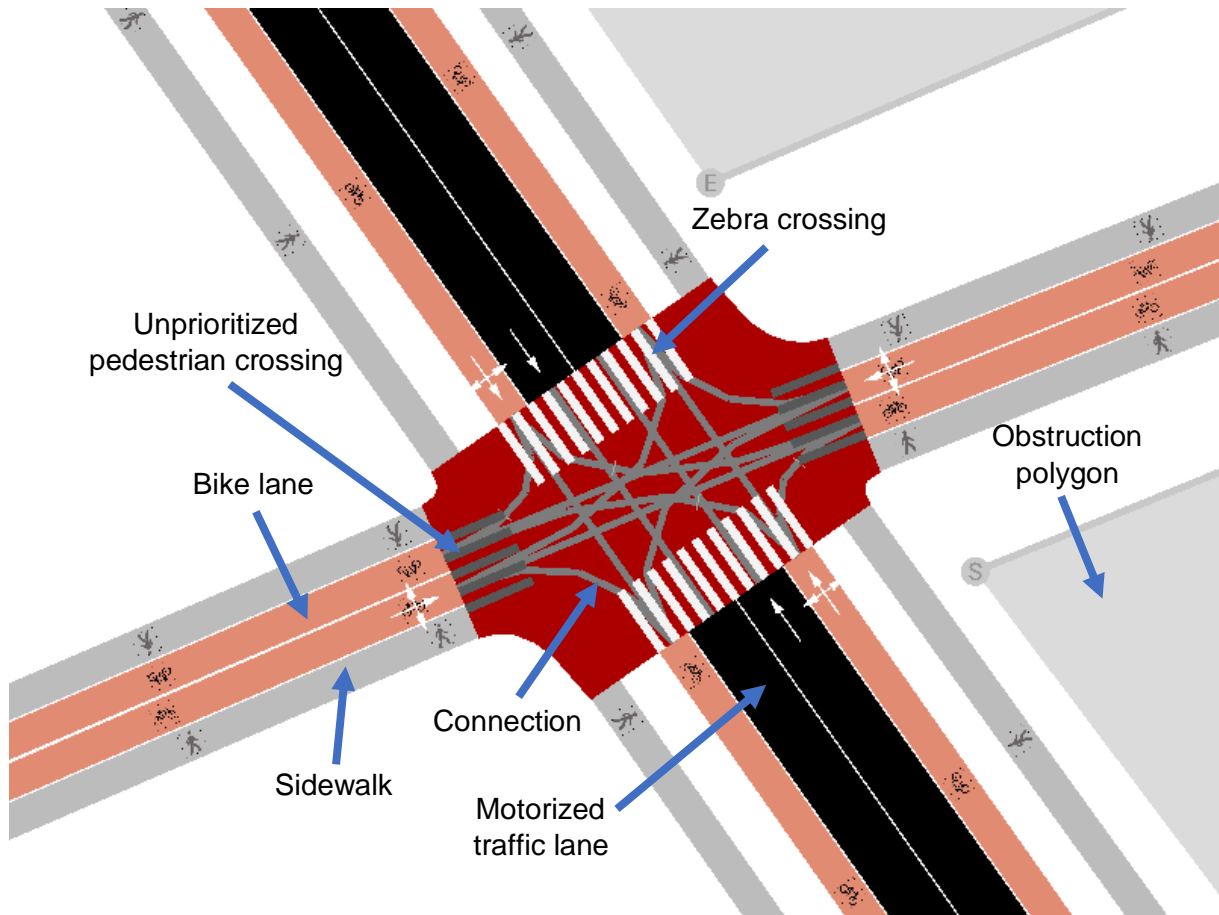


Figure 7 Part of the network with key components indicated.

5.2 The M4H network

What distinguishes this research from the others is the presence of buildings and other view obscuring elements. The proposed AV model takes the obstructed view caused by these objects into account when driving. The detailed map as provided in the spatial framework for the M4H in 2035 (*Toekomst in de Maak - Ruimtelijk Raamwerk Merwe-Vierhavensgebied Rotterdam*, 2019) was consulted to recreate the buildings and other obstructions in the simulated traffic network (Figure 7).

There are a total of 13 exit and entrance points, 12 of them are for disturbance traffic and one is exclusively for AVs. Of course, not all entity types can enter or leave at all of these points. The entrance and exit points of each entity type are shown in Figure 8. The entrance and exit points are weighted according to an assumed traffic inflow and outflow rate, the weights are presented in Table 4.

Table 4 Vehicle weights at entrance and exit points.

Entrance/exit point	Cars	Trailers	Bikes	Pedestrians
1	-	-	1	-
2	-	-	1	-
3	1	1	1	1
4	0.5	1	1	1
5	1	1	0.5	1
6	-	-	1	1
7	-	-	2	-
8	-	-	1	-
9	0.5	0.5	-	2
10	1	1	-	2
11	0.5	2	-	1
12	-	-	2	-

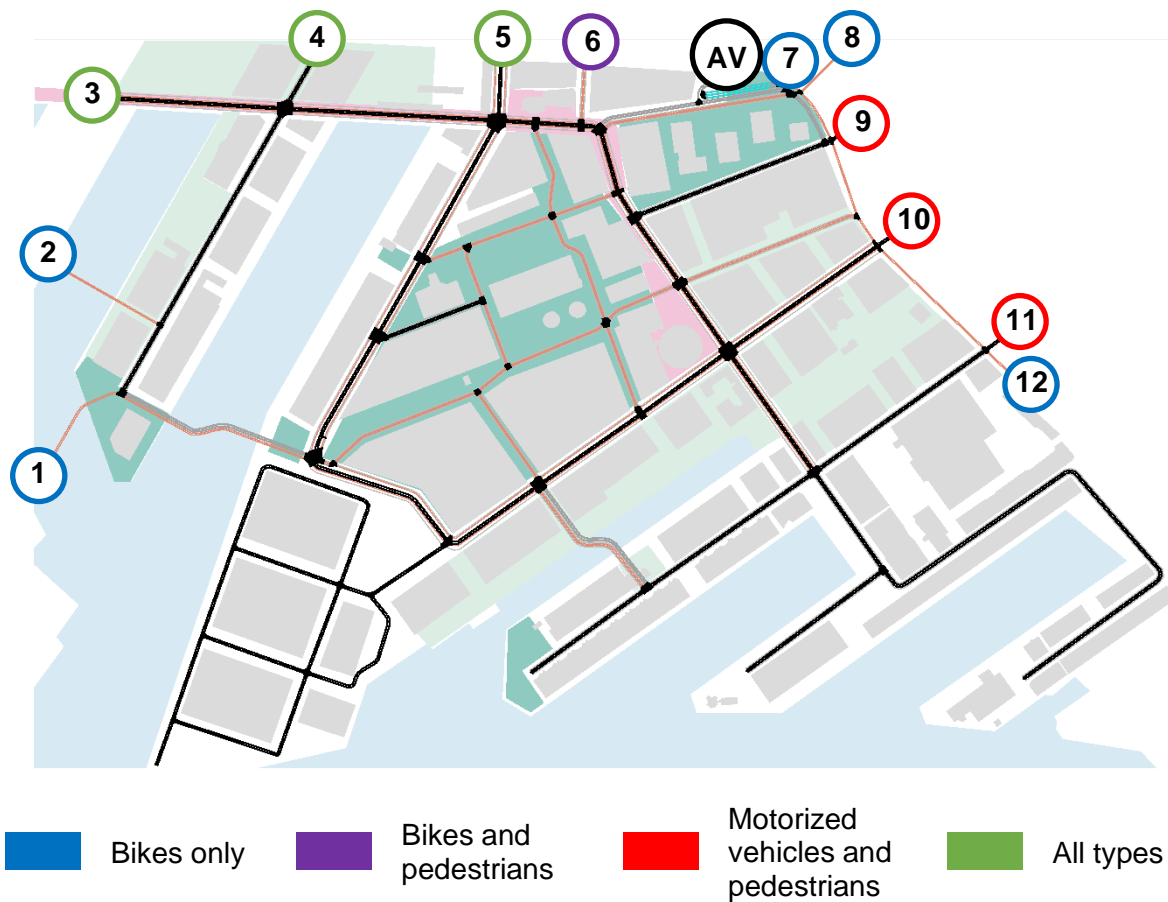


Figure 8 The complete network of M4H in 2035, with entrance and exit points indicated.

The original network has been slightly altered to accommodate the proposed AVs. They enter and exit the network in a platoon. When they enter, they immediately go to their delivery location. Since not all deliveries take the same amount of time, three buffer lanes at the AV exits haven been added to allow the AVs to reform their platoon (Figure 9).

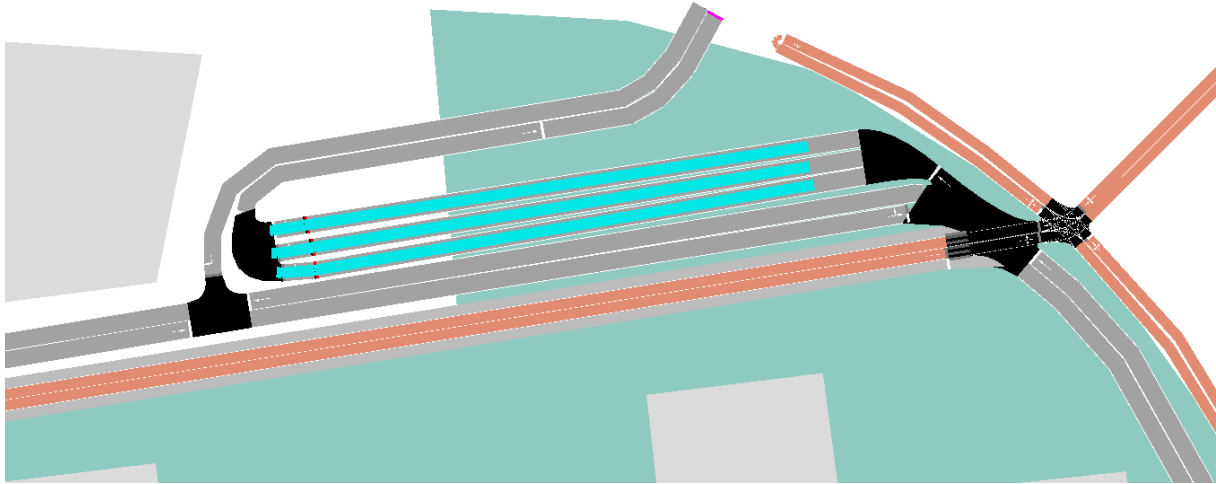


Figure 9 Platoon buffer lanes.

There are in total 6 possible delivery points for the AVs as indicated in Figure 10. These delivery points all have a weight of 1.

SUMO offers a built-in feature to add actuated traffic lights based on time gap in a network. In total five of those traffic lights have been added (Figure 11), four at the major four-way intersections, and one to regulate the inflow of AVs. By using actuated traffic lights, the traffic in the network is somewhat balanced resulting in a reduced risk of partly gridlocking the network while other parts are still uncongested.

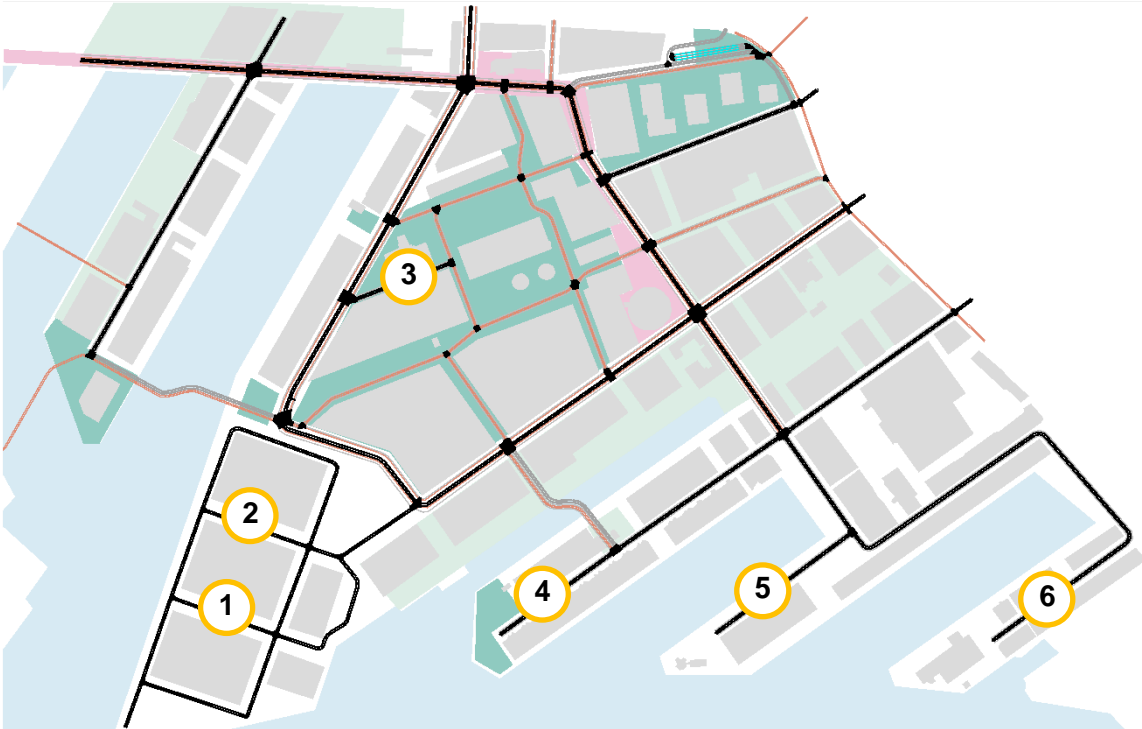


Figure 10 AV delivery points.

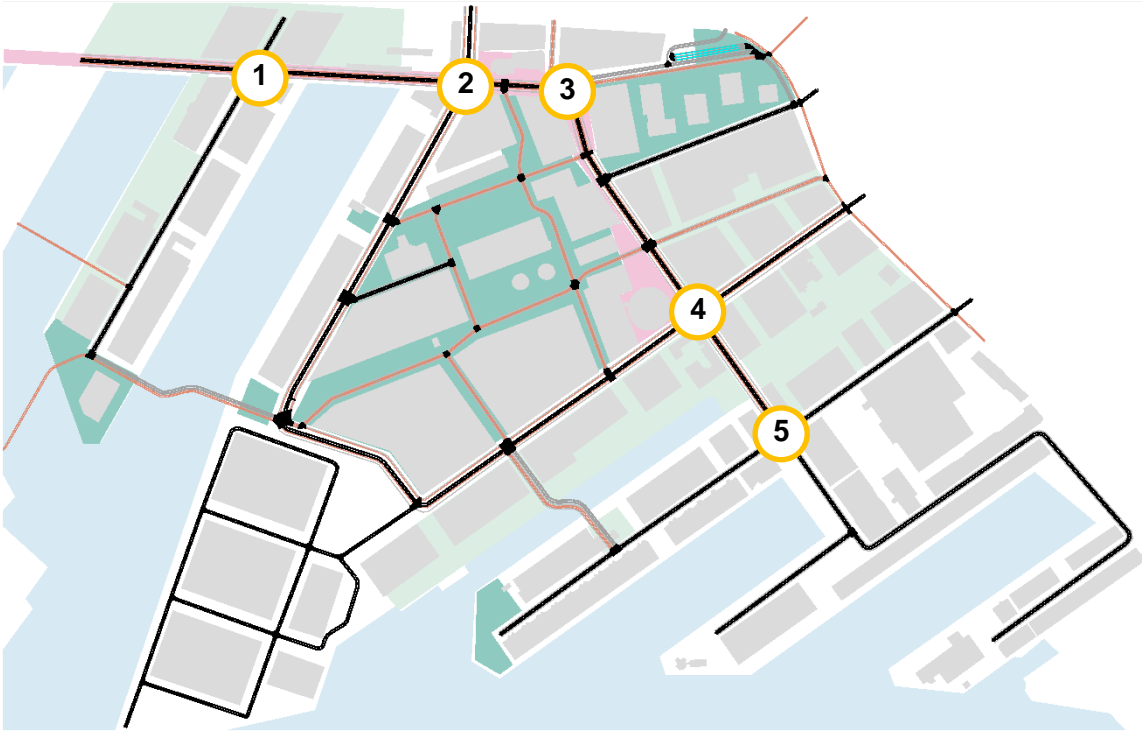


Figure 11 Locations of actuated traffic lights.

5.3 The simulated environment

In this subsection the simulation environment as used in the experiments is introduced. For all entities, the *duarouter* tool is used to generate all possible routes they can take (there are over 1400 different routes). At time of entity injection, a random route is chosen based on entrance, exit and demand point weights. First the way disturbance traffic is injected is discussed. Then, the AV platoon injection and management are explained.

5.3.1 Disturbance traffic

Since AVs are the main subjects in this research, other road users are considered disturbance traffic. A distinction is made between VRUs and normal road users. VRUs are cyclists and pedestrians, and normal road users are cars, trailers, and AVs. Other vehicle types like mopeds, motorcyclists and busses are not considered, since they can be represented by bicycles, cars, and trailers with only minor differences in characteristics. In Appendix A, Table 16 the default vehicle parameters are presented as used by SUMO version 1.7.0, the parameters of the AVs identical to the trailers.

The potential impact of emergency vehicles is not investigated. It is important that AVs are able to swerve and give way to these entities, but this is not considered for now. Additionally, no random actions like suddenly braking to avoid hitting birds, performing a U-turn on the middle of the road, being distracted by a mobile phone, swaying across lanes, etc. which could result in collisions are simulated.

Disturbance traffic is inserted at random Poisson distributed intervals. It is assumed that more critical conflicts happen at higher speeds. Therefore, the disturbance injection intervals are calibrated to be above a certain average vehicle speed. This way the simulated zone does not get too crowded and a low congestion state is guaranteed. The base number of vehicles per hour for the cars, trailers, bikes, and pedestrians are set to 130, 40, 70 and 70, respectively. It is assumed that this mix of traffic is sufficiently accurate for the purpose of this research. The aforementioned disturbance traffic ratio is always conserved but can be multiplied with the so-called *disturbance factor*. In the experiment the disturbance factor will gradually increase to generate the MFDs for different scenarios. Once the MFDs are generated a suitable *disturbance factor* range will be determined to assess the safety and time loss at low congested states.

5.3.2 AV management

At random Poisson distributed intervals, a platoon containing three to five AVs is injected into the simulation. About 40 AVs are released in the system every hour, to achieve this the injection system is instructed to inject a platoon every 360 seconds on average. Once a platoon is injected, the AVs will perform their last-mile delivery task individually. After executing their task, they will halt in the first free *platoon buffer lane* to be reunited with the other AVs to form a platoon again. The *AV dispatching system* recognizes AVs with the help of induction loops in the buffer lanes. If all expected AVs are in the lane and standing still, the platoon is ready to be released from the simulation. The traffic lights turn green and it moves towards the dedicated AV exit point.

5.4 Virtual AV model

In this subsection the virtual AV model is presented. The occlusion aware driving principle is explained first. Then, the speed controller logic of the AVs is introduced, and lastly the equipped SSI devices are presented.

5.4.1 Occlusion aware driving principle

What distinguishes this research from comparable microscopic traffic studies is the Occlusion Aware Driving (OAD) principle. The AVs are programmed in such a way, that their visibility range gets obstructed by obstacles such as buildings. Of all entities within the AV's visibility range all information regarding position, speed, route, and intentions is assumed to be known. Because of high computing power requirements, view obstructions caused by other road users are not considered. If the view of the AV would be obstructed by a vehicle that is already on an intersection or in front of the AV, the AV would not be able to drive anyway. Hence, this trade-off between required computing power versus simulation speed was made. It is assumed that this only impacts the simulation results slightly.

Because of the obstructed view caused by buildings, the AV might not be able to see certain entities hidden in the obstructed areas which makes it possible for dangerous and even fatal situations to occur. To mitigate this problem, OAD considers imaginary entities at the border of the visibility range, instead of only considering visible entities. These imaginary entities are from now on called Pseudo Vehicles (PVs) and can be divided into two groups. The first group are static PVs, which are modelled as a vehicle with zero speed and no intention to drive off. The second group is called dynamic PVs, which are modelled as the vehicles that drive the maximum allowed lane speed and have no intention to brake. This way, the AV should never be overwhelmed if an entity which was previously behind an occlusion appears.

In Figure 12 an AV in the simulation is shown with all relevant elements indicated. From this figure it becomes clear that generally only one static PV on the AV trajectory is considered, but several dynamic PVs are present. A dynamic PV is not just one entity with one route, but all possible routes allowed to be taken need to be considered by the *AV speed controller logic*. Although this adds a lot of complexity which greatly increases the required computing power, it is an essential part of the OAD logic. To reduce required computing power, a lookup table with the lidar polygons and PV objects is available.

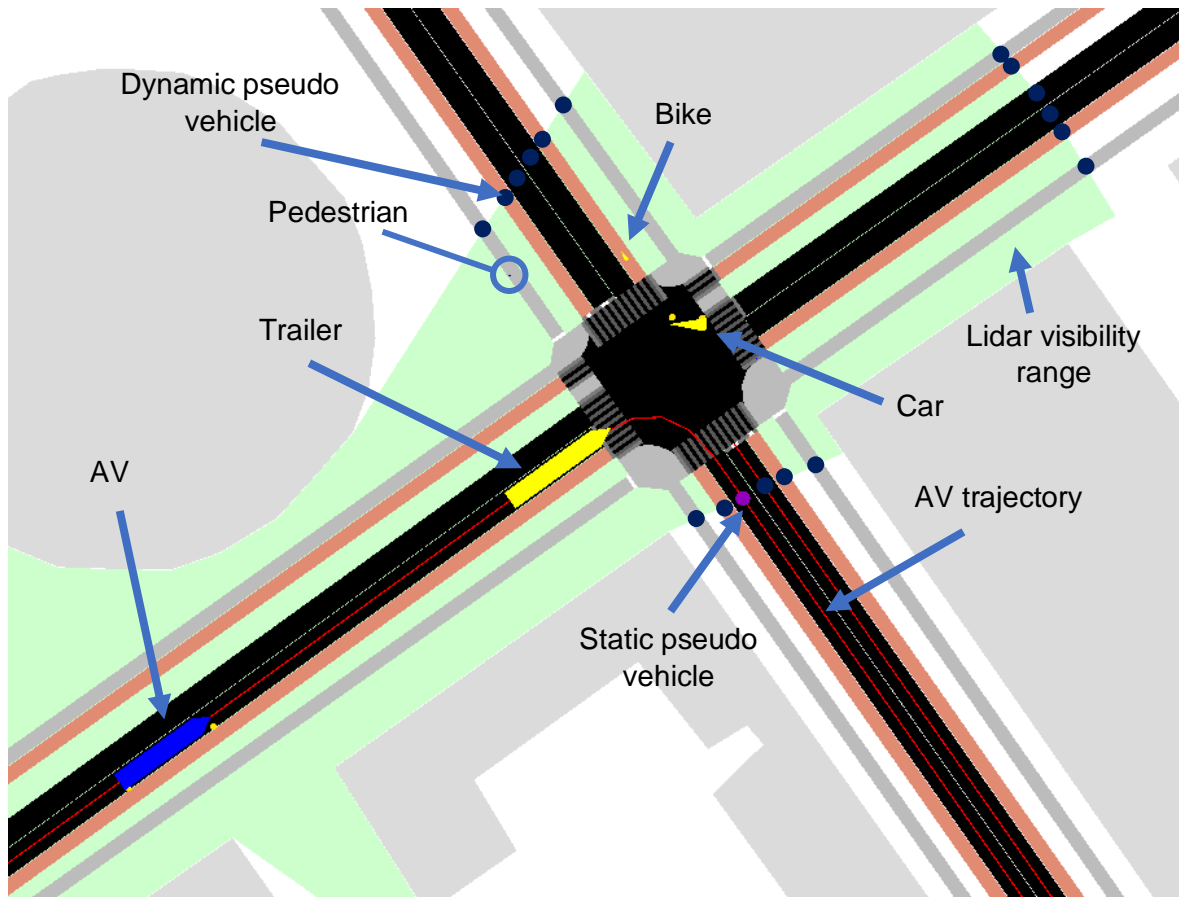


Figure 12 AV with all relevant elements indicated.

5.4.2 AV speed controller logic

This sub-subsection is based on, and adapted from earlier work of Pauwels (2020). To control the speed of the AVs, the *AV speed controller* is introduced. Lane keeping, steering, and determining the next position of the AV is managed by SUMO, the speed of AVs is controlled by the *speed controller* logic. It calculates the desired speed of the AV based on three models. The first model is the *car-following model*. It estimates the space gap between the AV and a vehicle in front, and calculates the required speed for the AV to respect the set time gap. The second model is the *junction model* that consists of decision logic to respect traffic rules (stopping for traffic lights, giving way, etc.) and determines whether it is safe for the AV to cross the intersection. It also calculates the speed it should take to be able to stop in time if it is not safe to cross the junction. The third model is the *pedestrian model*. It is focused on safe operation at pedestrian crossings. It makes sure that the AV does not collide with pedestrians and respects zebra crossings. When the safe speeds for all entities are calculated, the speed controller takes the minimum calculated speed as in equation (5.1) and instructs the AV to accelerate, decelerate or hold its speed. It also takes the maximum AV and allowed road speed into consideration.

$$v_{desired} = \min \begin{bmatrix} v_{max,road} \\ v_{max,AV} \\ v_{safe_j,vehicle_1} \\ v_{safe_{cf},vehicle_1} \\ v_{safe_{p,ped_1}} \\ \vdots \\ v_{safe_j,vehicle_n} \\ v_{safe_{cf},vehicle_n} \\ v_{safe_{pm,ped_n}} \end{bmatrix} \quad 5.1$$

Car-following model

The task of the car-following model is to prevent collisions with leading vehicles in following situations. It does this by keeping a constant time gap (τ) from the leading. Adaptive Cruise Control (ACC) systems make use of car-following models to estimate the safe following speed. Most manufacturers do not specify which model they use as they consider it a trade secret. If no intervehicular communication is available, there are no differences between AVs and vehicles with ACC in a leader-follower situation. Therefore, the same car-following models are applicable.

Various car-following models are available in SUMO, an overview is available on the SUMO wiki ("SUMO - Definition of Vehicles, Vehicle Types, and Routes," 2020). The Krauß car-following model (Krauß, 1998) is chosen for this application. The safe speed of the vehicle in the next simulation step is calculated with equation (5.2). The bumper to bumper gap is determined by drawing the AV trajectory and measuring the length of the segments between the AV and the leading vehicle. The leading vehicle's speed is assumed to be available.

In related work on AV research using SUMO (Lu et al., 2018; Lu et al., 2019) this car following model is also used. It is suspected that they used sub-second simulation steps as their desired time gap for AVs is set as low as 0.6 seconds. One must understand that this time gap is compensating for the reaction time of the AV. As the simulation step size is the lowest reaction time possible, time gaps lower than the simulation step size are undesirable and can result in collisions if the leader suddenly brakes. The simulation step size used in this research is 1 second, therefore the minimum stable value for the time gap is 1 second.

$$v_{safe_{cf},vehicle_n} = v_{vehicle_n} + \frac{g_{AV,vehicle_n} - v_{vehicle_n} \cdot \tau_{AV}}{\frac{v_{AV} + v_{vehicle_n}}{2 \cdot b_{AV}} + \tau_{AV}} \quad 5.2$$

where:

- v_x : Speed of x [$m \cdot s^{-1}$]
- $g_{x,y}$: Gap between x and y [m]
- τ_x : Time gap of x [s]
- b_x : Maximum deceleration rate of x [$m \cdot s^{-2}$]

Junction model

The junction model manages the behavior of the AV when approaching an intersection. At signalized intersections, the model does not have to consider a lot of entities, but at unsignalized intersections the junction model has to consider lots of factors. The task of a junction model is to prevent collisions and respect traffic rules. The difference with this junction

model and the standard model in SUMO is that this logic is from the AV's point of view, whereas the SUMO model is created from the junction's perspective.

It is clear to human drivers what the intentions of other road users are, but this is non-trivial for autonomous driving algorithms. In the survey of Yurtsever et al. (2020) on the state-of-art of autonomous driving systems (ADS), the recent developments of human driver intention prediction are presented. It states that researchers also focus on recognizing the individual driving styles of disturbance vehicles and suggests that it is a promising direction in ADS developments. This is because the possibility for driverless systems to recognize turn signals is already proven (Casares et al., 2012; Sathya et al., 2015). With the recent developments on intention prediction, it is assumed that the connection an observed vehicle takes on an intersection is predictable by the AV in 2035. Additionally, the driving speed of the disturbance vehicles is assumed to be available to the AV.

The decision scheme as shown in Figure 13 is the main logic behind the junction model. This logic must be followed for each disturbance vehicle and all intersections in the braking distance range of the AV as long as the outcome for the previous intersection is "go". If the outcome for junction k and vehicle n is "stop", the safe speed of the AV with respect to junction k is set to the maximum safe speed to brake in time (equations (5.3) and (5.4)) and subsequent junctions do not have to be checked.

$$v_{safe_{jk,vehicle_n}} = \begin{cases} v_{braking_{jk}}, & \text{if stop} \\ \infty, & \text{if go} \end{cases} \quad 5.3$$

The maximum safe speed for the AV to brake in time for junction k is calculated using equation (5.4) (simplified Krauß method). Note that the junction approaching speed is influenced by the desired time gap (τ_{AV}) of the AV.

$$v_{braking_{jk}} = \frac{g_{jk,AV} - minGap_{jk}}{\frac{v_{AV}}{2 \cdot b_{AV}} + \tau_{AV}} \quad 5.4$$

where:

$minGap_{jk}$: Minimum gap between AV and junction [m]

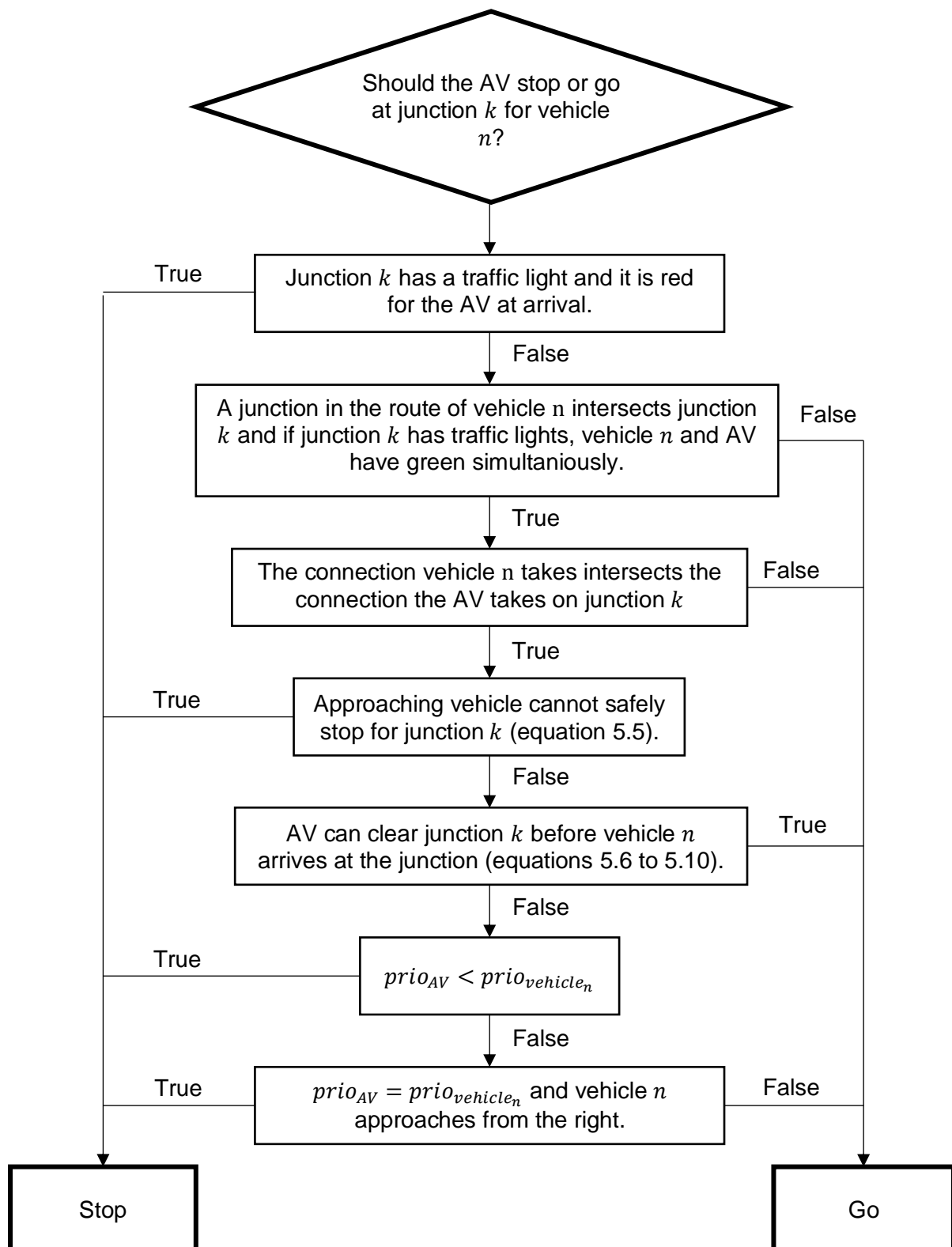


Figure 13 Junction model decision logic

The stopping distance of vehicle n is computed by equation 5.5. If this distance is greater than the distance to the junction, the approaching vehicle cannot safely stop.

$$s_{stopn} = \frac{v_{AV}^2}{2 \cdot b_{AV}} \quad 5.5$$

To estimate the arrival time of vehicle n at junction k equations (5.6) to (5.10) are used. These calculations can only be used if there are no other junctions between vehicle n and junction k or if the maximum allowed lane speed for all lanes on the trajectory are the same. If this is not the case, the arrival time for junction $k + 1$ is calculated by first calculating the end speed (v_{end}) at junction k and setting v_x to this value. Note that $g_{jk+1,x}$ needs to be set to the length of the approaching lane of junction $k + 1$ plus the connection length at junction k .

First, the speed difference between the current speed and allowed lane speed is calculated by equation (5.6).

$$\Delta v = v_{allowed} - v_x \quad 5.6$$

where:

$v_{allowed}$: Maximum allowed speed at approaching lane [$\text{m}\cdot\text{s}^{-1}$]

Equation (5.7) determines the time it takes to accelerate or decelerate to this new speed.

$$t_{acc} = \begin{cases} \frac{\Delta v}{a_x}, & \Delta v > 0 \\ \frac{\Delta v}{b_x}, & \Delta v \leq 0 \end{cases} \quad 5.7$$

where:

a_x : Maximum acceleration rate of x [$\text{m}\cdot\text{s}^{-2}$]

Acceleration or deceleration distance is calculated by equation (5.8). This is necessary to determine whether the vehicle is done with accelerating or decelerating before it reaches the junction.

$$s_{acc} = \begin{cases} v_x t_{acc} + \frac{a_x t_{acc}^2}{2}, & \Delta v > 0 \\ v_x t_{acc} - \frac{d_x t_{acc}^2}{2}, & \Delta v \leq 0 \end{cases} \quad 5.8$$

The approximated arrival time at junction k is calculated using formula (5.9). To calculate the junction clear time (t_{clear}), the same calculations can be used with the connection length at junction k and the vehicle length added to $g_{jk,x}$.

$$t_{arrival} = \begin{cases} \frac{g_{jk,x} - s_{acc}}{v_{allowed}} + t_{acc}, & g_{jk,x} - s_{acc} \geq 0 \\ \max \left(\frac{-v_x \pm \sqrt{v_x^2 + 2ag_{jk,x}}}{a} \right), & g_{jk,x} - s_{acc} < 0 \text{ and } \Delta v > 0 \\ \max \left(\frac{v_x \pm \sqrt{v_x^2 - 2dg_{jk,x}}}{d} \right), & g_{jk,x} - s_{acc} < 0 \text{ and } \Delta v \leq 0 \end{cases} \quad 5.9$$

where:

$g_{jk,x}$: Gap between junction k and x [m]

Finally, the speed at the end of the given gap is calculated by equation (5.10).

$$v_{end} = \begin{cases} v_{allowed}, & g_{jk,x} - s_{acc} \geq 0 \\ t_{arrival} * a_x + v_x, & g_{jk,x} - s_{acc} < 0 \text{ and } \Delta v > 0 \\ -t_{arrival} * b_x + v_x, & g_{jk,x} - s_{acc} < 0 \text{ and } \Delta v \leq 0 \end{cases} \quad 5.10$$

Pedestrian model

Due to limitations of SUMO, pedestrians can only cross roads at dedicated crossings which are located at junctions. As mentioned earlier, a distinction is made between prioritized and unprioritized crossings (Figure 7). The pedestrian model can be considered as a part of the junction model; but because of the different calculations and logic, a distinction is made between the two.

In Figure 14, the decision scheme of the pedestrian model is given. Note that the arrival and clear time of the AV are calculated with equations (5.6) to (5.10). To prevent congestion on the junction, the allowed braking distance considered by the AV is the distance to the junction, which is not necessarily the distance to the crossing. To calculate accurate arrival and clear times for the pedestrian, equations (5.11) and (5.12) are used. Acceleration and deceleration rates of the pedestrians are very high in comparison to their maximum speed. Therefore, the calculations are simplified for the pedestrians. It is assumed that they can go from a standstill to maximum speed instantly and vice versa.

The pedestrian model only has to be checked if the junction model for junction k has resulted in “go”. If so, for each pedestrian and crossing on the junction the pedestrian model is evaluated. When the outcome of the decision scheme for a crossing on junction k is “stop”, the safe speed ($v_{safe_{pm,ped_p}}$) is set to the maximum speed for the AV to brake in time for junction k , which is calculated by equation (5.4).

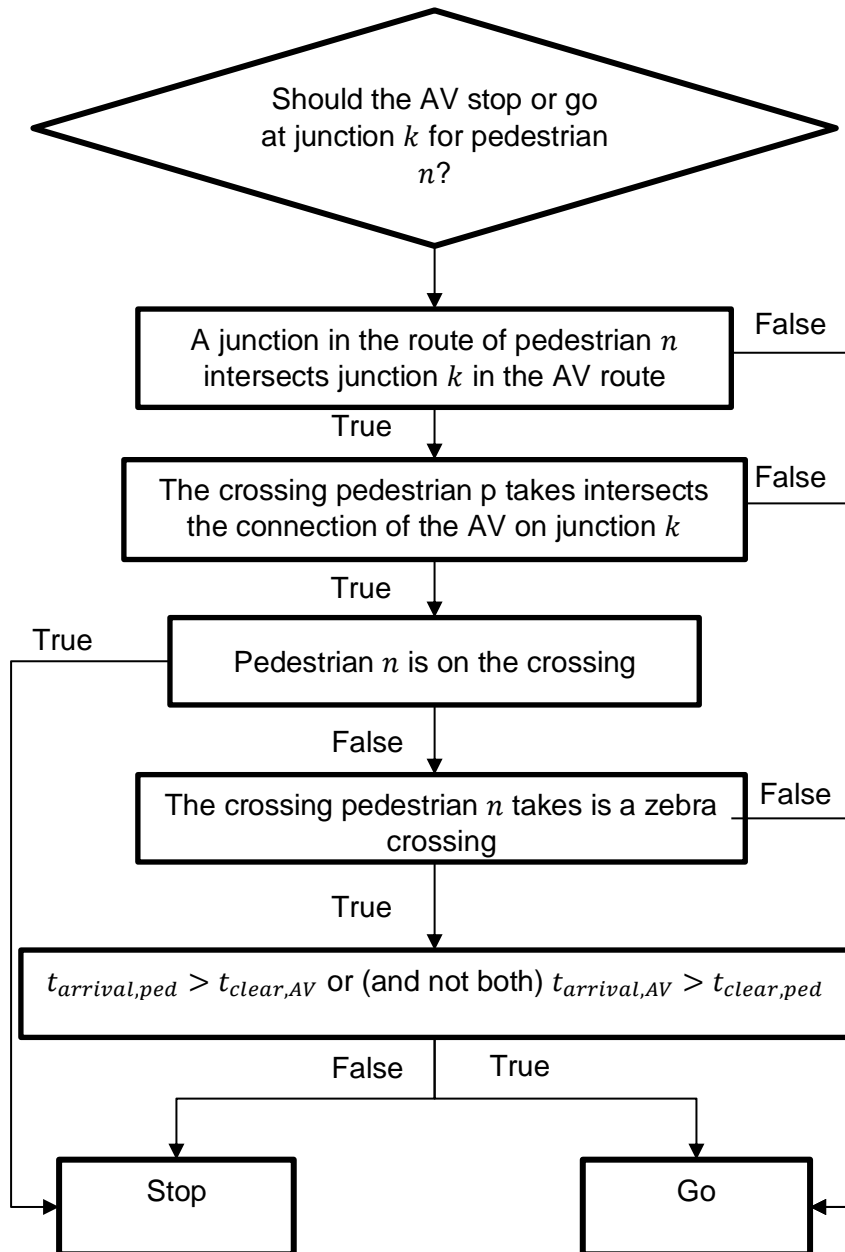


Figure 14 Pedestrian model decision logic

$$t_{arrival,ped} = \frac{g_{crossing,ped}}{v_{max,ped}} = TTZ_{ped} \quad 5.11$$

Where:

 $g_{crossing,ped}$: Gap between crossing and x [m]

$$t_{clear,ped} = \frac{g_{crossing,ped} + w_{crossing}}{v_{max,ped}} \quad 5.12$$

Where:

 $w_{crossing}$: Width of the crossing and x [m]

5.4.3 SSI devices

To evaluate the safety of the network, the AVs are outfitted with SSI devices. These devices record the time, position, speed, route, and estimate the conflict point location of the vehicles within a straight-line distance of 100 meters. The standard SUMO SSI devices calculate DRAC, TTC and PET only for vehicles, not pedestrians. These indicators are not considered sufficient to evaluate the actual safety of the system. For example, reaction times are not taken into account and crash severity is not estimated. Because the time, position, speed, and conflict points are logged, other indicators can be calculated after the simulation has finished. The additional calculated indicators are: STCT, TA, TIT, MTTC, CI, PSD, and CrF. When considering the STCT SSI, the level of seriousness is estimated by linear interpolation using Figure 5.

With the lack of pedestrian safety evaluation SSIs available in SUMO. An SSI device had to be created which logs the time, position, and route of the pedestrians within the straight-line distance of 100 meters. The same indicators are calculated, except for CS which has been substituted by the PRI. The PRI is a hybrid indicator that estimates both severity and crash rate for pedestrians.

The only evasive action that can be taken by the AV in this microsimulation environment is braking. Swerving and accelerating (above the speed limit) is not modelled. Estimating the exact moment of the evasive action is non-trivial in microsimulations (in real life, too). An acceptable threshold for determining whether a braking event is considered an evasive action, is a deceleration of more than $2 \text{ m}\cdot\text{s}^{-2}$ (Axelsson et al., 2016). This will be used to calculate the TA, STCT and other TA-based indicators.

6

Benchmark of the M4H

To verify the safety and efficiency evaluation methodology and to obtain a benchmark for the zone as it is designed now, multiple simulation scenarios are evaluated. In these scenarios the car-following time gap (τ) of the AVs is varied from 1 to 2.5 seconds with steps of 0.5. Note that this also affects the speed of the AVs when approaching junctions (section 5.4.2). For all scenarios, the same random seeds are used to ensure that the exact same traffic is injected. There will be two types of simulation sets.

The first set of simulations, each set consisting of 30 seeds and each seed running for 12.000 seconds (excluding 1.000 seconds warm-up time), are at low traffic densities. By doing this, more complicated interactions between AVs and other traffic components are expected compared to high densities. If the traffic density is high, the network is congested, and the AVs are simply following the vehicle in front until they reach an intersection and then decide at low speed how to act. Since the real network is almost never fully congested, it is believed that interactions at higher velocities and lower traffic densities are a better representation of the real network behavior. This first set of simulations is also used to evaluate the time loss caused by interaction with other traffic. Time loss is used to assess the operational efficiency of the AVs. It is thought that higher delays of the AVs cause other traffic partitioners to be more irritated resulting in a more aggressive driving style (Hennessy et al., 1999).

In the second set of simulations the traffic density is steadily increased until the network is sufficiently gridlocked. The traffic flow, average speed, and density are recorded and the MFDs are generated for all scenarios. Then, the MFDs are used to confirm that there are no large differences in network performance due to randomness between runs or any modelling errors. As the fraction of AVs gets small at higher traffic densities, it is believed that the MFDs should converge.

6.1 Safety benchmark

Before the first set of simulations can be assessed on safety, all potential accidents must be identified. This is done by calculating STCT, PET, and DRAC_{max} and subjecting them to the relaxed threshold values of Table 5. If one or more thresholds are violated, the incident is marked as a potential accident and it will be subjected to a full safety assessment. By using these three indicators, it is believed all typical safety critical situations are caught. STCT captures both the AV speed and time of the evasive actions. The PET indicator captures potentially critical conflicts without evasive actions. Finally, DRAC gives insight in the required braking capability. Time, distance, and deceleration is considered by judging all conflicts with

these SSIs. This preselection makes sure that the severity of a non-critical conflicts is not calculated. The thresholds are obtained by taking commonly used thresholds (Table 6) and relaxing them. If tighter thresholds were to be used, it is possible that STCT, PET, and DRAC_{max} report the conflict as non-critical, while other SSIs might consider it to be critical.

Table 5 SSI threshold values to determine if there is a potential accident.

SSI	Potential accident thresholds
STCT	> 21
PET	< 5
DRAC _{max}	> 2

Reasonable threshold values are set to determine if the potential accident should be marked as an actual accident. Potential accidents that violate the threshold for a certain SSI are reported as an accident for this SSI. Since the total number of incidents differ per scenario due to random chance, the number of accidents for a given SSI is divided by the total number of incidents of each scenario. The resulting fraction is used to compare the level of safety.

The used threshold values are presented in Table 6. Threshold values for STCT, TTC_{min}, TA, MTTC_{min}, PET, PSD_{min}, and DRAC_{max} come from literature (chapter 3), some adjustments are made to capture more SII accidents. Again, note that there are no set thresholds that determine whether a situation is safe or unsafe. So, adjusting these thresholds to capture more SSI accidents is possible, which is actually common practice in related studies. CI_{max}, CrF_{max}, and PRI have no thresholds in literature because they describe the severity of conflicts. However, it is assumed the safety level can still be judged using thresholds. Thresholds to capture enough SSI accidents are determined by evaluating the obtained data. A similar approach is taken when determining a threshold for the TIT indicator. This way, the four indicators can still be useful for comparing the safety between different scenarios.

Table 6 SSI threshold values as used in the safety assessment.

SSI	Threshold		Comment
	Vehicles and bikes	Pedestrians	
STCT	> 25	> 25	One level safer than the original work (Laureshyn et al., 2018).
TTC _{min}	< 1.25	< 1.25	Commonly used (Mahmud et al., 2017).
TA	< 1.5	< 1.5	Commonly used (Mahmud et al., 2017).
TIT	> 0.35	> 0.35	Determined from data.
MTTC _{min}	< 4	< 3	Commonly used, slightly tighter for pedestrians. (Ozbay et al., 2008)
CI _{max}	> 10	-	Determined from data.
PET	< 3	< 3	Slightly tighter (Alhajyaseen, 2015).
PSD _{min}	< 1	< 1	Commonly used (Allen et al., 1978).
DRAC _{max}	> 2.5	> 2.5	Maximum braking acceleration, slightly tighter (Giuseppe Guido et al., 2012).
CrF _{max}	> 50	> 50	Determined from data.
PRI	-	> 0.1	Determined from data.

6.1.1 Results

All SSIs of potential accidents are calculated using the appropriate equations from section 3 and subjected to the thresholds from Table 6. The assessed incidents assessed involve AV-AV, AV-bike, AV-trailer, AV-car, and AV-pedestrian. The combined results for cars, trailers and bikes are presented first and in the second subsection the results for pedestrians are presented.

Vehicles and bikes

The obtained data regarding accidents involving AVs, vehicles and bikes as determined by the SSI assessment are presented in Table 7 and graphically in Figure 15. Nearly all indicators show a reduction in the number of accidents as the car-following time gap increases, except the SSIs PET and PSD.

Table 7 Results of the SSI assessment for vehicles and bikes.

Scenario	$\tau = 1$	$\tau = 1.5$	$\tau = 2$	$\tau = 2.5$
No. incidents	60376	58637	57455	57539
SSI	Percentage of accidents			
STCT	14.20%	11.96%	8.15%	2.81%
TTC _{min}	4.11%	3.58%	2.34%	0.00%
TA	7.49%	7.21%	6.72%	4.44%
TIT	3.43%	3.13%	0.87%	0.00%
MTTC _{min}	4.11%	3.53%	1.77%	0.56%
CI _{max}	3.49%	3.21%	1.50%	0.65%
PET	0.91%	0.97%	0.88%	0.93%
PSD _{min}	3.66%	2.31%	2.14%	2.27%
DRAC _{max}	4.92%	2.93%	0.43%	0.52%
CrF _{max}	4.06%	3.24%	2.11%	0.67%

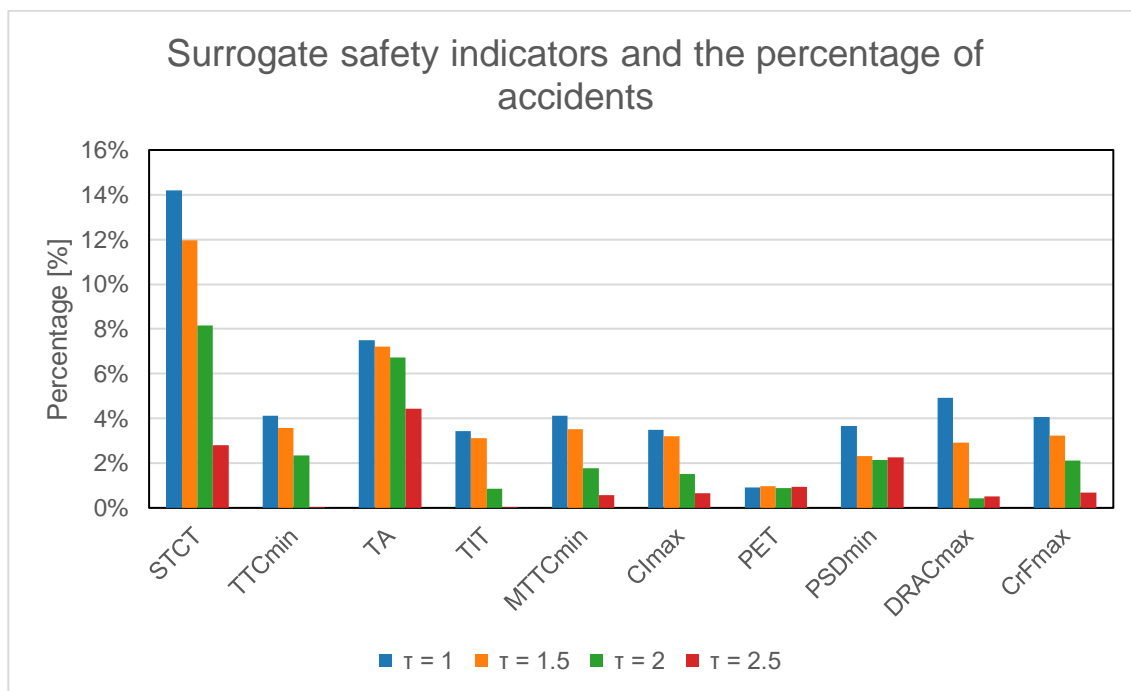


Figure 15 Graphical representation of the results of the SSI assessment for vehicles and bikes.

Pedestrians

The results of the SSI assessment involving AVs and pedestrians are presented in Table 8 and graphically in Figure 16. All SSIs show a decrease in accident frequency when the car-following time gap of the AV increases.

Table 8 Results of the SSI assessment for pedestrians.

Scenario	$\tau = 1$	$\tau = 1.5$	$\tau = 2$	$\tau = 2.5$
No. incidents	46777	47538	48545	49813
SSI	Percentage of accidents			
STCT	3.47%	2.23%	1.48%	1.15%
TTC _{min}	16.36%	14.90%	11.13%	9.52%
TA	1.85%	1.21%	0.90%	0.75%
TIT	15.60%	13.58%	10.11%	8.80%
MTTC _{min}	21.00%	18.14%	13.63%	11.81%
PET	1.96%	1.78%	1.66%	1.58%
PSD _{min}	6.17%	5.26%	3.56%	3.64%
DRAC _{max}	12.61%	9.01%	8.24%	7.50%
CrF _{max}	19.77%	15.93%	8.93%	7.64%
PRI	5.14%	3.09%	1.60%	1.11%

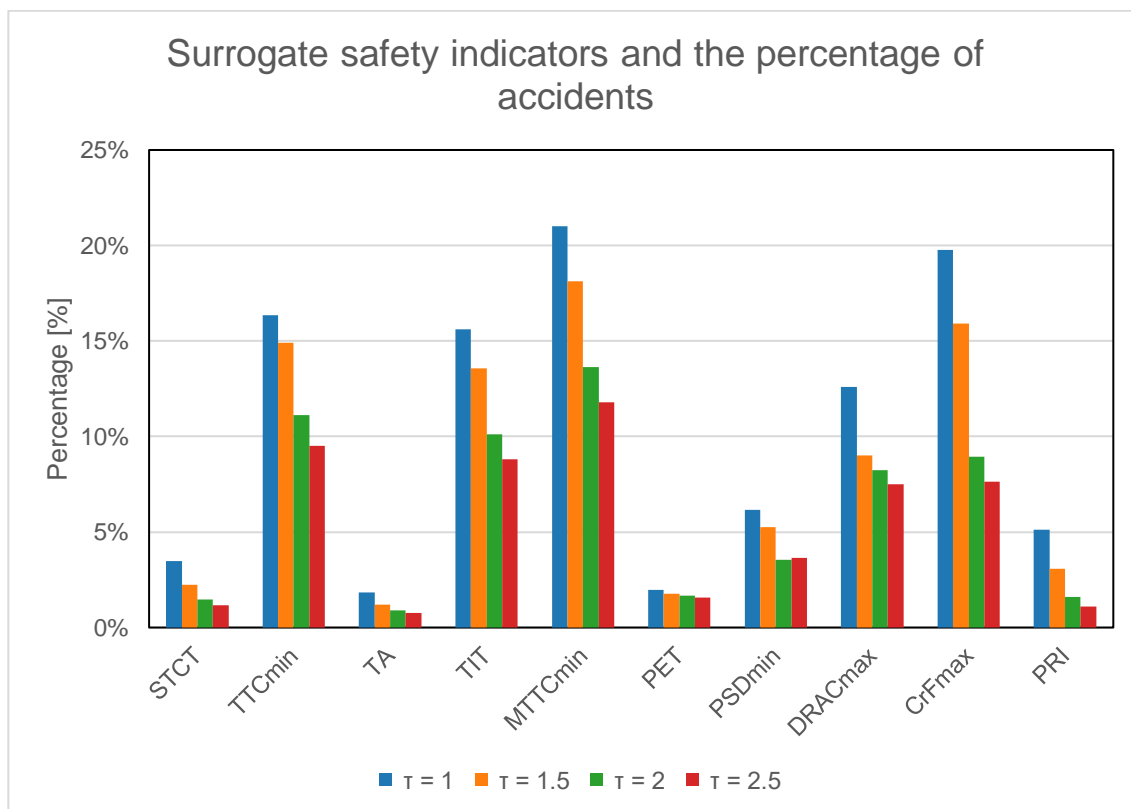


Figure 16 Graphical representation of the results of the SSI assessment for pedestrians.

6.2 Efficiency benchmark

With the second set of simulations, the MFDs for the different car-following time gaps are generated. The MFDs are used to evaluate the overall network performance of the scenarios and are generated using the data of the approaching lanes at locations 2 and 4 of the intersections with actuated traffic lights (Figure 11). Additionally, a scenario without AVs is simulated to investigate if a small ratio of AVs impacts the network performance. When generating the MFDs, the disturbance traffic is steadily increased, but the AV injection rate is constant. Therefore, with increasing traffic, the fraction of AVs gets smaller. It is suspected that in the low-density region, the effects of AVs are bigger and at higher density regions lower, resulting in converging MFDs at high traffic density states.

To evaluate the time loss of the vehicles under the scenarios, the free flow time of all routes is required. This is generated by injecting the appropriate vehicle three times for each route while there are no other vehicles in the system and taking the average time in the system. Since there are over 1400 possible routes and generating these free flow times takes substantial computation power, it was assumed that three repetitions would be sufficiently accurate. For the AVs, the time-following gap was set to 2 seconds when generating the free flow times. The first set of simulation results is used to calculate the time loss fraction. Due to the random impact of traffic lights, it is possible that the time in system of certain entities is lower than the free flow time. Note that the time loss of pedestrians is not considered.

6.2.1 Results

MFD

Figure 17 shows the MFDs of all scenarios; for comparison, a scenario without AVs was also added. From the density-flow and speed-flow diagram, it is observed that the scattered flow rates become chaotic at higher vehicle densities and lower average speeds, respectively. Interestingly enough, the density-speed diagram shows a relation with little scatter for all densities and speed compared to the other diagrams. In general, no major differences in MFDs are observed. In low scatter regions, the MFDs are almost identical and in higher scatter regions the uncertainty gets too high to be meaningful. In Appendix B, Figure 24 the flow, speed and densities obtained from the first set of simulations are plotted in the MFDs from Figure 17.

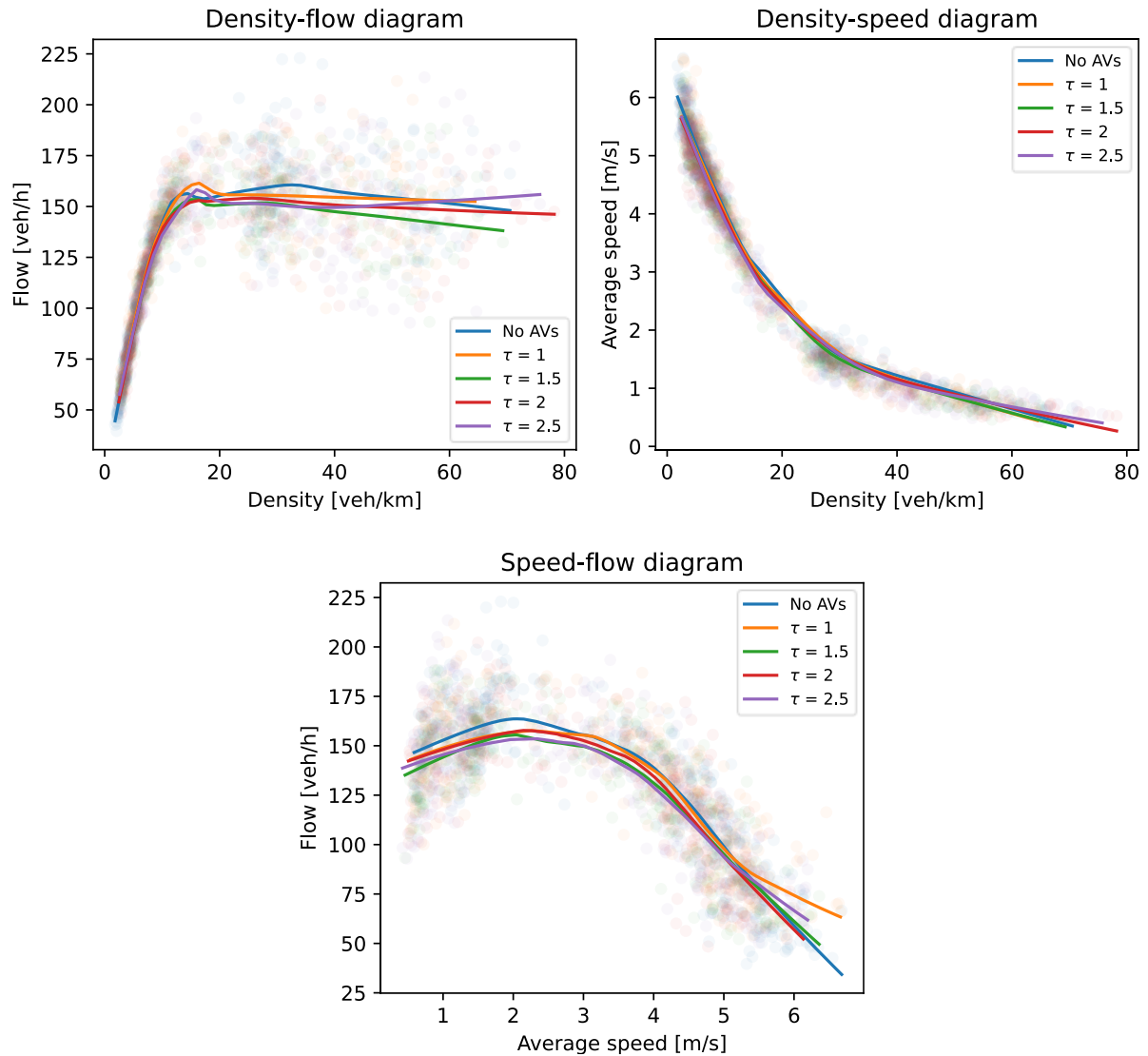


Figure 17 MFD of the benchmark scenarios.

Time loss

The results of the time loss analysis are presented as a boxplot in Figure 18 and the average delays are presented in Table 9. It is observed that the introduction of AVs increases the delay of all vehicles. The time loss of the AVs gets significantly higher as the car-following time gap increases (Table 9). Bikes do not show a change in delay by the varying car-following parameter. Cars seem to be slightly influenced by the more conservative driving of the AVs, which is confirmed by the t-test (Table 10). Trailers show an increase in delay caused by the car-following parameters of the AVs, but the H_0 cannot be rejected.

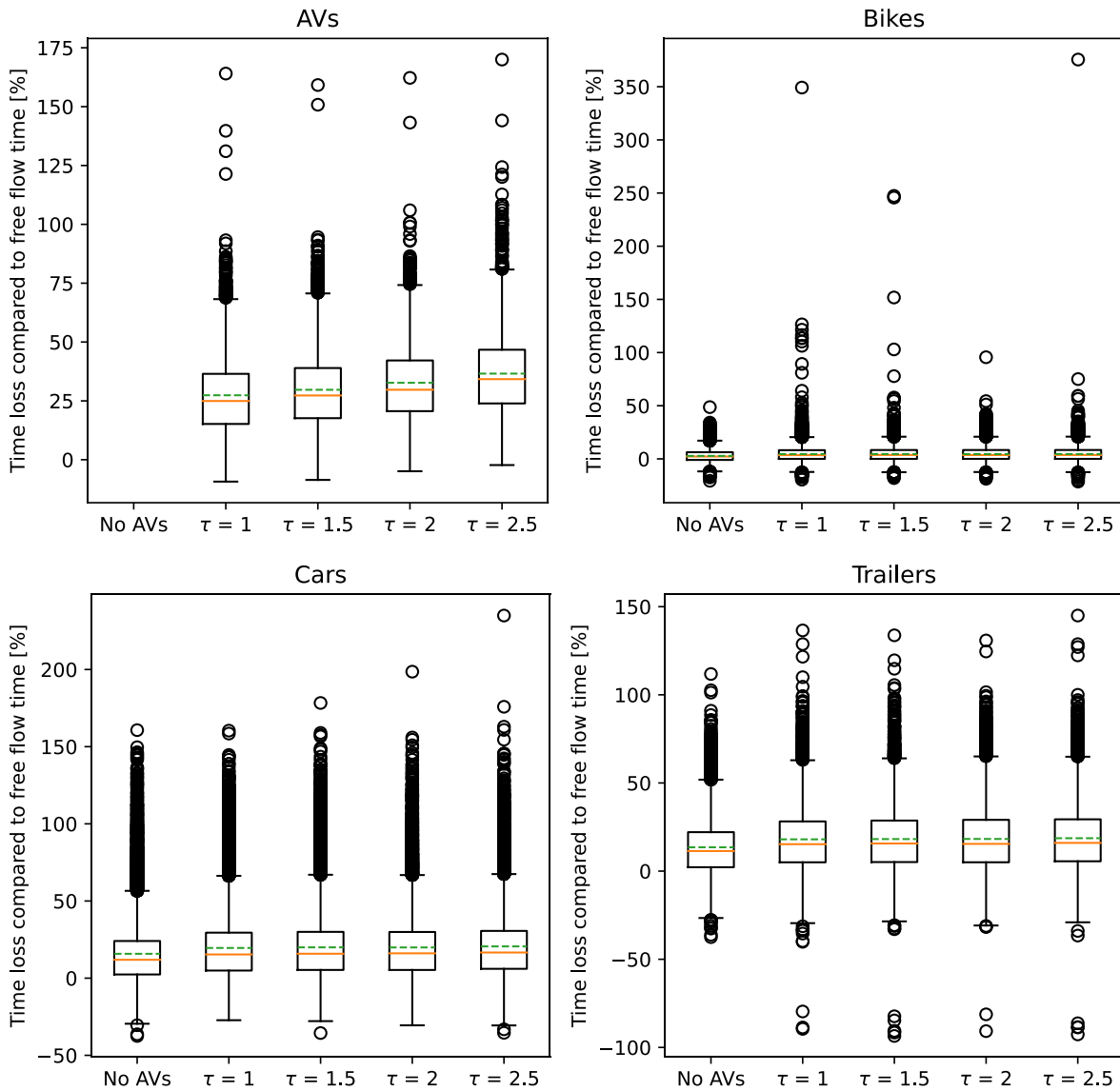


Figure 18 Boxplots of the time loss percentage compared to free flow times per entity.

Table 9 The average percentage of delay compared to free-flowing vehicles.

Entity	No AVs	$\tau = 1$	$\tau = 1.5$	$\tau = 2$	$\tau = 2.5$
AVs	-	27.4%	29.7%	32.7%	36.6%
Bikes	2.8%	4.6%	4.6%	4.5%	4.6%
Cars	15.8%	19.6%	20.0%	19.9%	20.6%
Trailers	13.5%	18.0%	18.2%	18.2%	18.7%

Table 10 Results of independent t-test for delays of car-following time gap 1 and 2.5 seconds.

Entity	P-value	H ₀ rejected (p < 0.05)
AVs	4.45 x 10 ⁻¹¹⁵	Yes
Bikes	0.865	No
Cars	3.63 x 10 ⁻⁶	Yes
Trailers	6.05 x 10 ⁻²	No

6.3 Discussion

In the previous subsection, a benchmark of the performance of the simulation model was created. This was done by running two sets of simulations. The first set kept the number of vehicles in the simulation constant and recorded the interactions. This was used to calculate SSIs and time loss compared to free-flowing vehicles. In the second set, the amount of disturbance traffic was steadily increased to a congested state. This set was initially used to generate MFDs. So, it could be confirmed that there are no large differences in network performance due to randomness between runs or any modeling errors. Although there is a fairly large scatter, the MFDs are considered sufficiently similar to conclude that a small fraction of AVs does not have an unrealistically large effect on the network performance. The MFDs are actually so similar, that the introduction of AVs may not have an impact on the MFD at all.

It was observed that with increasing car-following time gap, the number and severity of accidents decreased according to most SSIs for AV-AV, AV-trailers, AV-cars, and AV-bikes interactions. The frequency of accidents for the PET and PSD SSIs did not or only slightly decrease. This can be caused by the disturbance vehicles instead of the AV, imperfections in the AVs driving model, or that they are simply not affected by the car-following time gap.

The SSI assessment for AV-pedestrian interaction shows promising results. All SSIs decreased with increasing car-following time gap. The reductions in accidents is probably more profound in the pedestrian assessment since there is only one type of conflict (crossing). The PET decreased less than the other SSIs, which is likely caused by the same reasons as in the previous paragraph.

From the time loss analysis, it is obvious that the introduction of AVs increases the delay of all vehicles. This can be because the AVs were just left out, resulting in fewer disturbance vehicles, and thereby lowering the level of service (LOS). To prevent this unfair comparison, the AVs could have been substituted by trailers. In Appendix B Figure 24 the flow, speed and densities obtained from the first set of simulations are plotted in the MFDs from Figure 18. The speed-flow diagram indeed hints towards a lower LOS for the no AVs scenario. If the reduced delays would indeed be caused by the lower LOS, the similarities in MFDs for the no AVs scenario compared to all other scenarios are justified.

Furthermore, the results show that the time loss of the AVs gets higher as the car-following time gap increases. Cars are for certain slightly influenced by the more conservative driving of the AVs. For trailers this could not be confirmed but it is suspected. Longer delays could be dangerous as it could provoke aggressive driving behavior towards AVs resulting in less safe driving. The bikes did not show any change in delay by the varying car-following parameter.

This is probably because they are mostly separated from other traffic in their own dedicated lanes.

In short, there is strong evidence that there exists a trade-off between safety and efficiency when varying the car-following parameters. It is proven that the safety and efficiency analysis methods are sensitive enough to be influenced by driving parameters and possibly by safety measures. In the next chapter, the AV's desired time gap is set to 2 seconds, and the safety and operational efficiency results from this section are used for further investigation.

7

Measures and impact on safety and efficiency

From the benchmark, it is known that the AVs are subjected to critical safety situations and vehicle delays. In an effort to improve safety and reduce vehicle delays, five possible measures are investigated. Three of the five measures are communication-based: V2V, V2I, and V2X. The other two measures are infrastructural based: reducing the maximum allowed speed and keeping a certain area around intersections clear of obstructions. As the OAD principle should guarantee safe driving behavior in simulated environments, the safety parameters are not expected to change between scenarios.

For each measure, a simulation scenario is created. Like the benchmark (chapter 6), two sets of simulation results are used for each scenario. The first set is used to evaluate the SSIs and time loss of the entities. This is done by simulating the network at low traffic densities for 12.000 seconds (excluding 1000 seconds warm up) for 30 different seeds, where the same seeds are used for each scenario. In the second set, the number of disturbance vehicles is steadily increased until the network is sufficiently gridlocked. During these simulations the traffic flow, density and average speed are recorded and the MFDs are created.

7.1 Possible measures

As mentioned earlier, five scenarios will be evaluated on their level of safety and operational efficiency, and compared to the previously obtained benchmark. In Table 11, the different scenarios are listed and their variation compared to the benchmark is explained. It should be noted that introducing V2V communication between AVs is relatively cheap as it only requires an extra communication device on the AVs. The additional static sensors in the V2I scenario add range to the AVs at busy interactions and can collect valuable data of the traffic, but they are more expensive than V2V. An advantage of V2I is that there are always sensors present at a location, with V2V it depends on whether there are other AVs around.

Table 11 The different simulation scenarios and their variation on the benchmark.

Scenario	Variation
Benchmark	Default AV model, with car-following time gap of 2 seconds.
V2V	When V2V is enabled and the lidar polygons of two or more AVs intersect (the V2V communication range is the lidar range), the knowledge of all visible disturbance vehicles gets combined and obsolete pseudo vehicles get removed. Information of other AVs outside the lidar range is not be useful as the AV cannot rule out any pseudo vehicles. If the AV is following another AV, a shorter car-following time gap of 1 second is set for the car-following model, the junction model will be left as is. Since disturbance vehicles will most likely not have V2V communication systems, only AVs are considered to have V2V available.
V2I	At the busiest and most occluded intersections in the zone, static lidars are placed (Figure 19) to observe entities in the same way AVs do. When the polygons of static lidar(s) and an AV intersect, the information the static lidar has on disturbance vehicles is send to the AV. Note that the AV does not (!) send its information back to the static lidars, this would result an undesirable limited type of V2V. With the combined information on disturbance vehicles, obsolete pseudo vehicles can be removed.
V2X	Combines the principles of V2V and V2I.
Slow Down (SD)	Certain non-arterial lanes are subjected to a lower speed limit. By default all AV/trailer/car lanes have a speed limit of 50 km/h, the lanes colored blue in Figure 19 are limited to 30 km/h.
Keep Clear (KC)	In an effort to reduce unnecessary conservative behavior of the AVs, building closer than 10 meters to intersections is forbidden. By doing this, the view of the AV should be less obstructed allowing it to approach junctions at higher (safe) velocities.

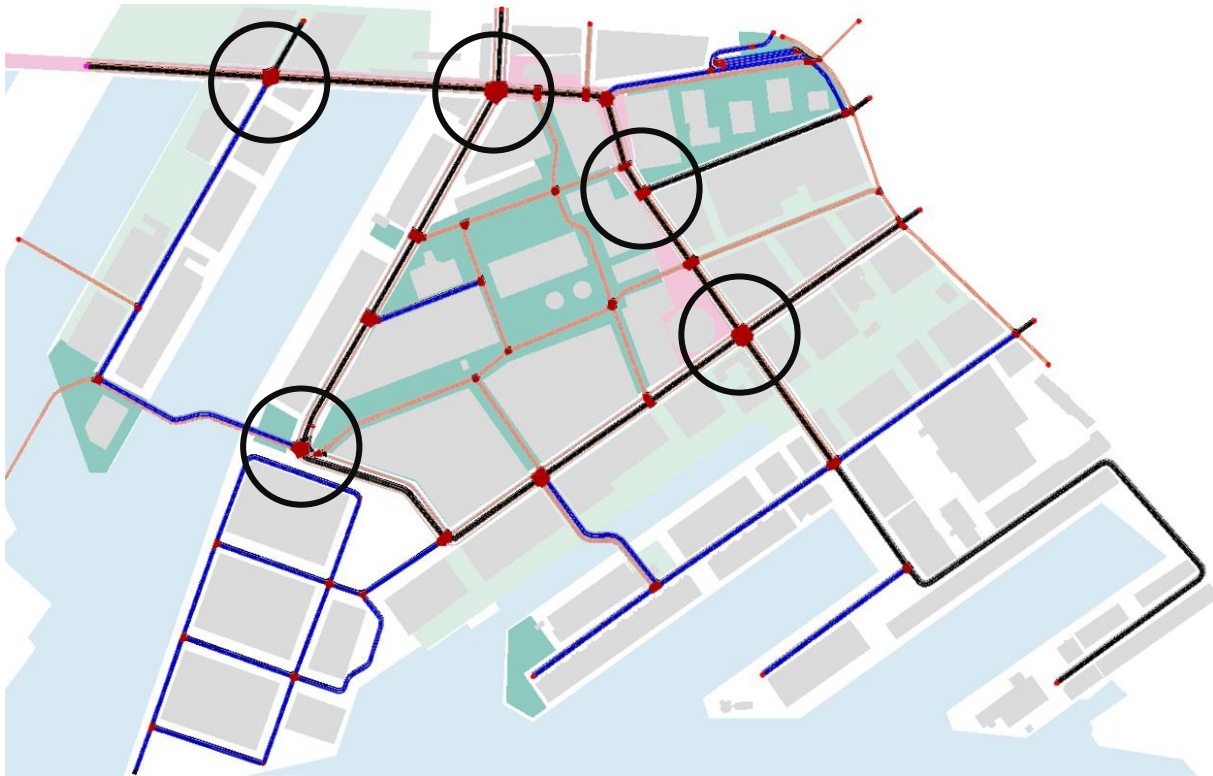


Figure 19 The M4H network with static lidar positions indicated with a black circle and the lower speed limit lanes colored blue.

7.2 Safety results

Safety is assessed in the same way as in the benchmark in chapter 6. Using the pre-selection thresholds presented in Table 6 the potential accidents are identified. All SSIs of potential accidents are calculated using the appropriate equations from section 3 and subjected to the thresholds from Table 6. The incident types assessed are AV-AV, AV-bike, AV-trailer, AV-car, and AV-pedestrian. The combined results for cars, trailers and bikes are presented first. In the second subsection the results for pedestrians are presented.

7.2.1 Vehicles

The obtained data regarding accidents involving AVs, vehicles and bikes as determined by the SSI assessment are presented in Table 12 and graphically in Figure 20. For the V2I, V2V, V2X and KC scenarios there is either a slight increase or a slight decrease in accidents according to the SSIs. It is observed in the SD scenario that there is a reduction in the recorded number of accidents for all SSIs, except MTTC and PET. MTTC is higher in the SD scenario compared to the benchmark and PET about equal.

Table 12 Results of the SSI assessment for vehicles and bikes.

Scenario	Bench	V2I	V2V	V2X	SD	KC
No. incidents	57455	56154	52976	56143	54534	57366
SSI	Percentage of accidents					
STCT	8.15%	8.22%	8.07%	8.70%	1.06%	8.40%
TTC _{min}	2.34%	1.83%	2.21%	2.02%	0.00%	2.38%
TA	6.72%	7.05%	6.36%	6.93%	5.51%	6.96%
TIT	0.87%	1.05%	0.58%	1.04%	0.00%	1.16%
MTTC _{min}	1.77%	2.08%	1.87%	1.66%	4.37%	1.73%
CI _{max}	1.50%	2.02%	1.66%	1.26%	1.19%	1.70%
PET	0.88%	0.92%	0.86%	0.83%	0.87%	0.87%
PSD _{min}	2.14%	2.06%	2.11%	2.73%	1.78%	2.03%
DRAC _{max}	0.43%	0.43%	0.46%	0.50%	0.34%	0.36%
CrF _{max}	2.11%	1.92%	1.92%	3.16%	0.00%	2.04%

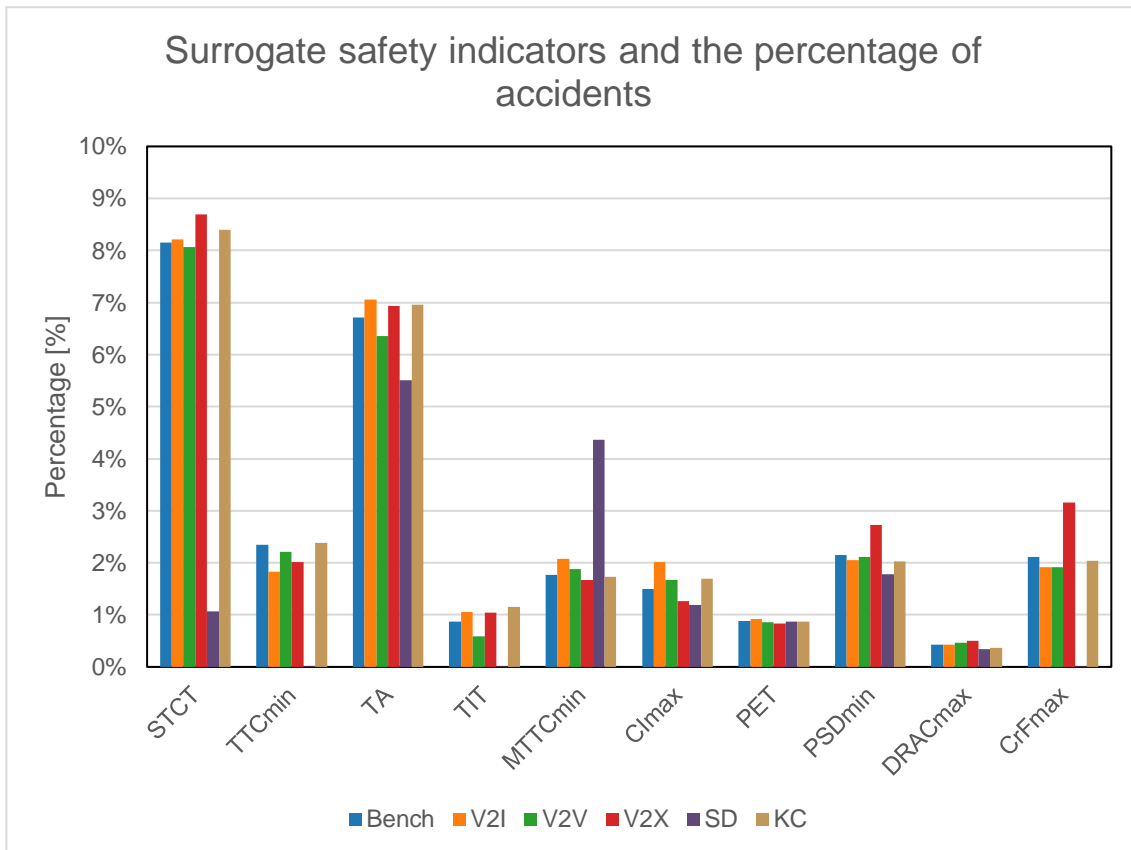


Figure 20 Graphical representation of the results of the SSI assessment for vehicles and bikes.

7.2.2 Pedestrians

The results of the SSI assessment involving AVs and pedestrians are presented in Table 13 and graphically in Figure 21. All SSIs are relatively equal or higher compared to the benchmark for the scenarios V2I, V2V, V2X and KC. For the SD scenario the reported accidents according to the SSIs are about equal or lower than the benchmark.

Table 13 Results of the SSI assessment for pedestrians.

Scenario	Bench	V2I	V2V	V2X	SD	KC
No. incidents	48545	51343	54165	58156	48198	47945
SSI	Percentage of accidents					
STCT	1.48%	1.73%	1.57%	1.62%	1.35%	1.61%
TTC _{min}	11.13%	14.75%	12.74%	15.13%	10.83%	13.33%
TA	0.90%	0.96%	0.92%	0.89%	1.00%	0.99%
TIT	10.11%	13.37%	11.93%	13.88%	10.15%	12.22%
MTTC _{min}	13.63%	17.94%	15.78%	18.74%	12.91%	17.20%
PET	1.66%	1.52%	1.32%	1.29%	1.69%	1.86%
PSD _{min}	3.56%	6.23%	4.98%	6.68%	2.37%	4.10%
DRAC _{max}	8.24%	12.22%	10.12%	13.02%	7.00%	9.62%
CrF _{max}	8.93%	13.29%	10.96%	14.19%	7.06%	10.88%
PRI	1.60%	1.63%	1.45%	1.60%	1.40%	2.01%

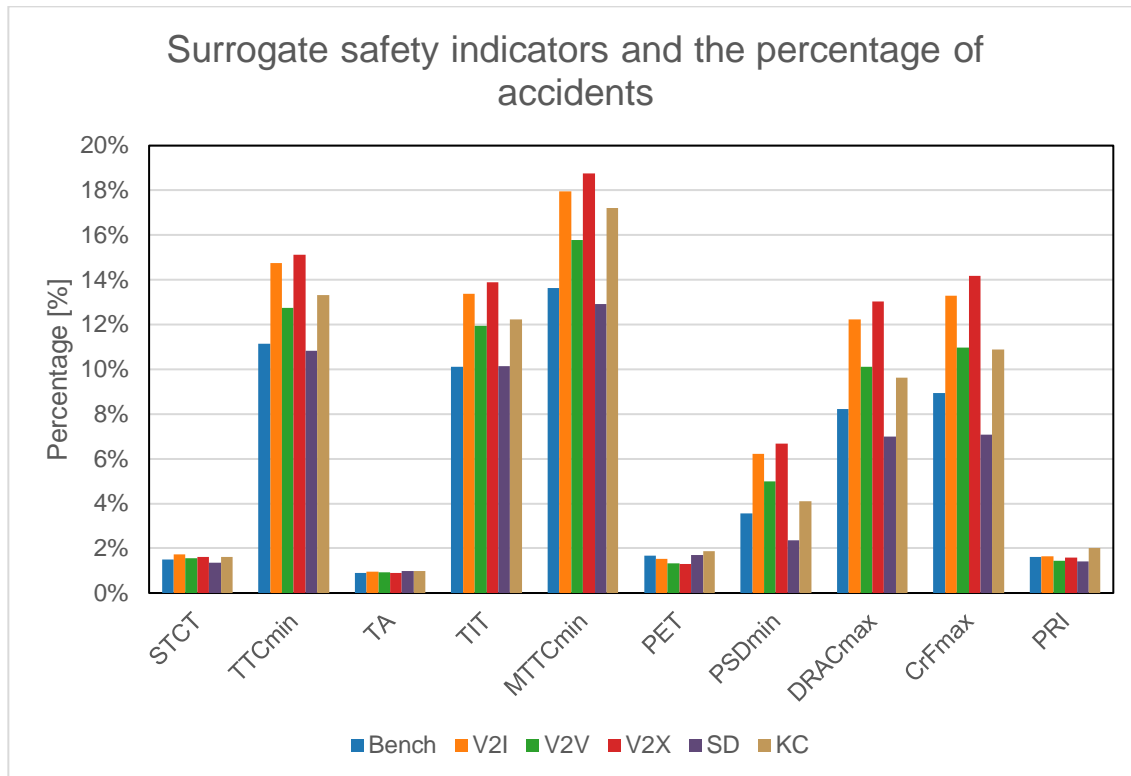


Figure 21 Graphical representation of the results of the SSI assessment for pedestrians.

7.3 Efficiency results

The efficiency assessment consists of two parts. In the first part MFDs are generated with the second set of simulation results using the traffic data of the approaching lanes at location 2 and 4 of the intersections with actuated traffic lights (Figure 11). This is done to catch any potential modelling errors and to verify that there are no large differences in network performance due to randomness between runs. In the second part the average time loss (delay) fraction is calculated using the first set of stimulation results. Note that the time loss of pedestrians is not considered.

7.3.1 MFD

The MFDs for all simulation scenarios are presented in Figure 22. For compassion, a no AV scenario is added again. At higher vehicle densities and lower average speeds, the scattered flow rate become more chaotic in the density-flow and speed-flow diagram, respectively. The density-speed diagram shows a relation with little scatter across the whole spectrum. In the low scatter regions, the MFDs of the scenarios are almost identical, while in higher scatter regions the uncertainty is high. In Appendix C, Figure 25 the flow, speed and densities obtained from the first set of simulations are plotted in the MFDs from Figure 22.

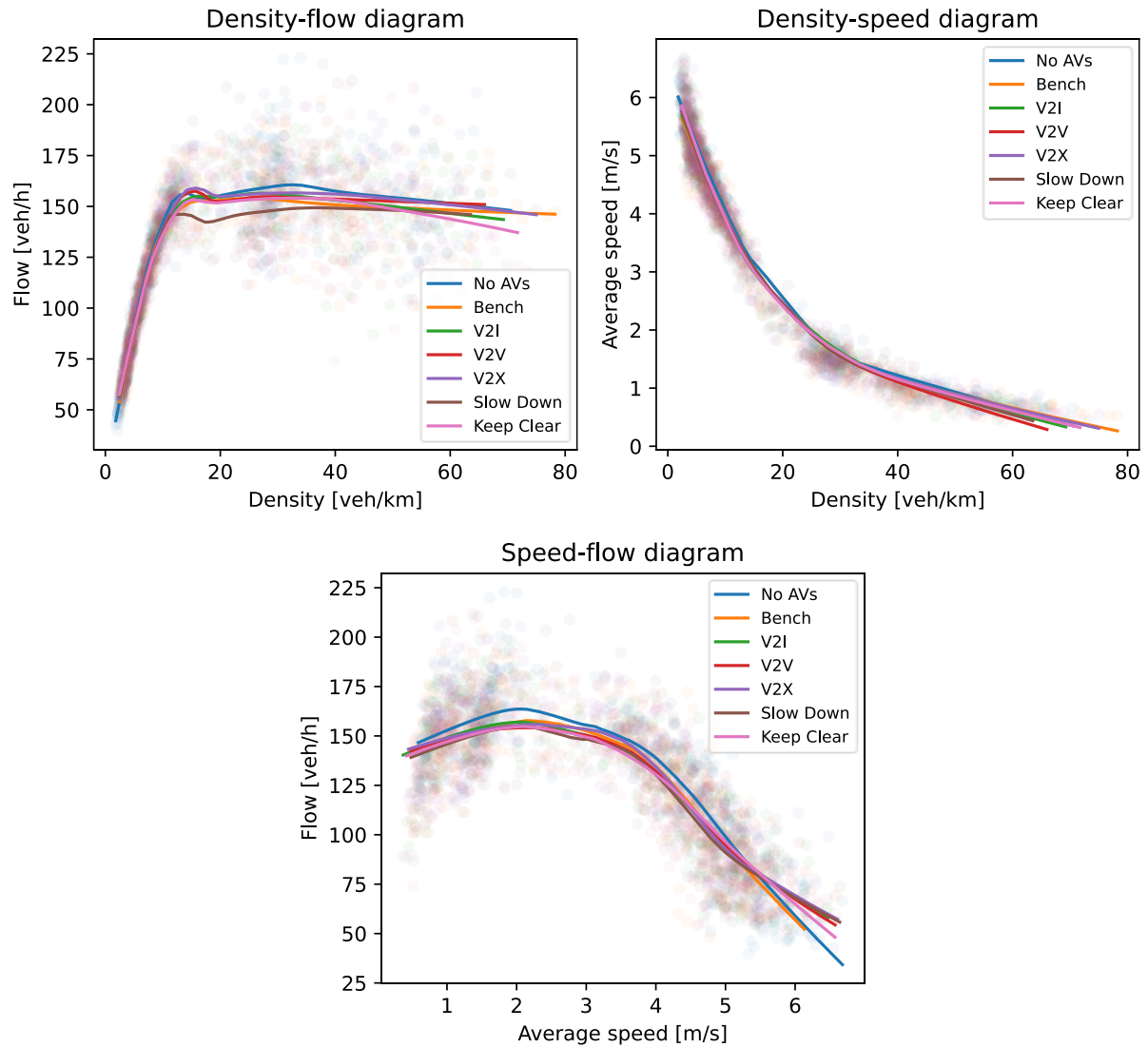


Figure 22 MFD of scenarios with measures.

7.3.2 Time loss

The fraction of time in system and free flow time of all vehicles for the different scenarios are presented as a boxplot in Figure 23. Table 14 shows the performance gain, i.e. the reduction of time loss, compared to the benchmark scenario. In Table 15, the results of an independent t-test comparing the time loss fractions of each scenario to the benchmark are presented.

It is observed that the AVs experience a significant (H_0 rejected) and fairly large performance boost in the V2I, V2V, V2X and KC scenarios. Other entity types do not seem to be significantly affected in these scenarios. All vehicles are significantly affected in the SD scenario, resulting in a worse performance for this scenario.

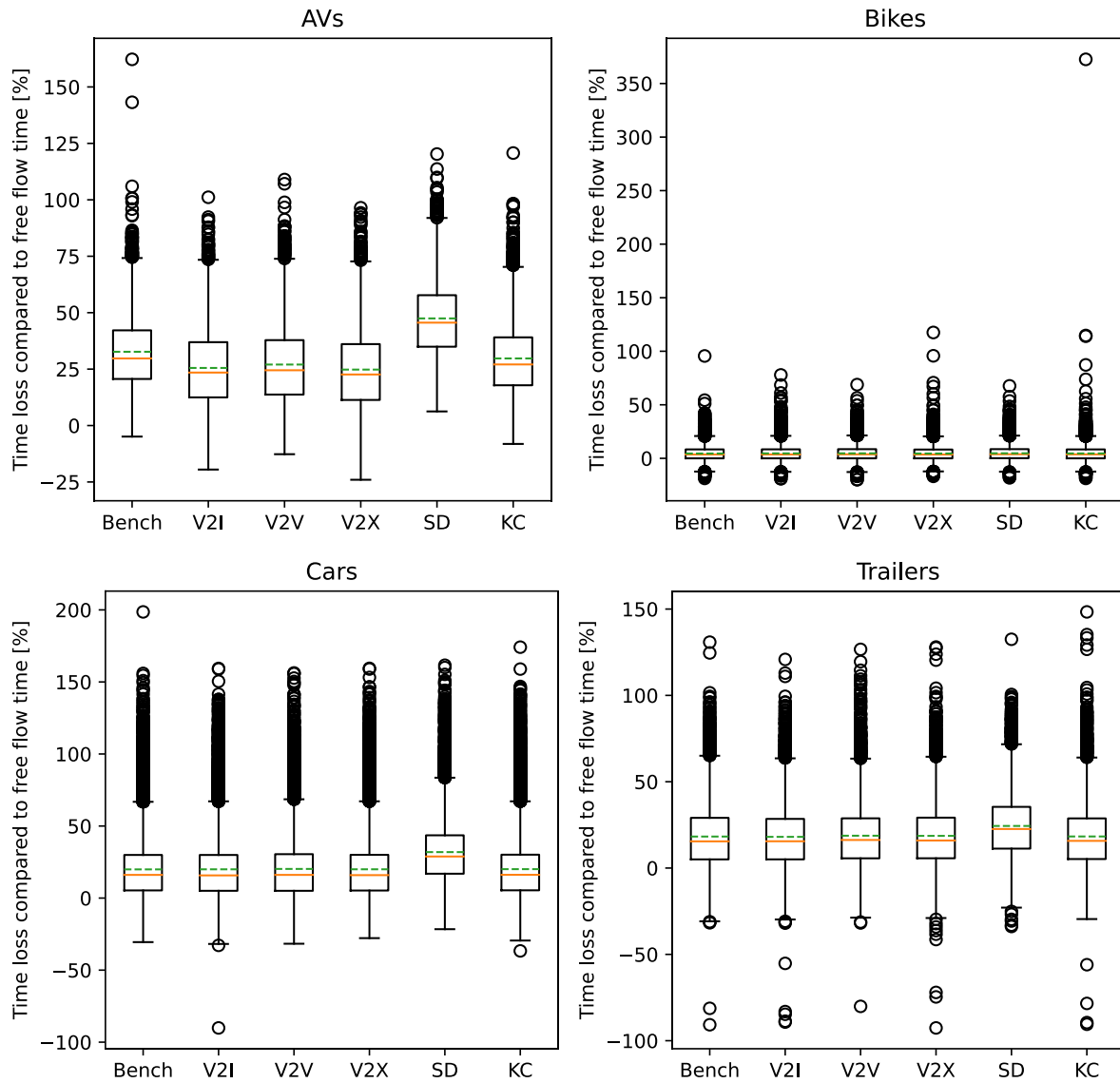


Figure 23 Boxplots of the time loss percentage compared to free flow times per entity.

Table 14 Performance gain (reduction of average time loss fraction) compared to the benchmark.

Entity	V2I	V2V	V2X	SD	KC
AVs	+7.2%	+6.3%	+7.9%	-14.8%	+3.0%
Bikes	-0.1%	-0.1%	0.0%	-0.2%	-0.1%
Cars	-0.1%	-0.1%	+0.4%	-12.0%	-0.2%
Trailers	+0.1%	-0.3%	-0.1%	-6.2%	-0.1%

Table 15 Results of independent t-test for delays of the benchmark compared to the scenarios.

Scenario		AVs	Bikes	Cars	Trailers
V2I	P-value	$6,60 \times 10^{-71}$	0,215	0,846	0,595
	H0 rejected ($p < 0.05$)	Yes	No	No	No
V2V	P-value	$4,16 \times 10^{-51}$	0,476	0,555	0,377
	H0 rejected ($p < 0.05$)	Yes	No	No	No
V2X	P-value	$1,73 \times 10^{-78}$	0,967	0,089	0,962
	H0 rejected ($p < 0.05$)	Yes	No	No	No
SD	P-value	$1,8 \times 10^{-292}$	2.75×10^{-2}	0	$4,16 \times 10^{-71}$
	H0 rejected ($p < 0.05$)	Yes	Yes	Yes	Yes
KC	P-value	$1,29 \times 10^{-14}$	0,460	0,467	0,883
	H0 rejected ($p < 0.05$)	Yes	No	No	No

7.4 Discussion

In this chapter several measures to improve safety and/or operational efficiency were introduced and investigated. Five measures were investigated of which three were communication based: V2I, V2V and V2X. The other two were infrastructural based: reducing the maximum allowed speed and keeping a certain area around intersections clear of obstructions. For all measures, a simulation scenario was created, and two sets of simulation results were generated.

The first set of simulations kept the number of vehicles constant and recorded all conflict involving AVs. These conflicts were used to calculate the SSIs and the average time loss of the entities was determined. In the second simulation set, the number of disturbance entities was steadily increased until the network was in a congested state. This set was used to generate MFDs so it could be confirmed that there are no large differences in network performance due to randomness between runs or any modelling errors. Although there is a fairly large scatter, the MFDs are considered sufficiently similar to conclude that a small fraction of AVs does not have an unrealistically large effect on the network performance. The MFDs are actually so similar, that the introduction of AVs may not have an impact on the MFD at all.

The results of the safety assessment for AV-AV, AV-trailer, AV-car, and AV-bike interactions showed that for the V2I, V2V, V2X and KC scenarios there is either a slight increase or a slight decrease in accidents according to the SSIs. This was actually expected since the OAD method should guarantee safe driving behavior in simulated environments. Again, with the introduction of PVs, collisions should never happen at the cost of operational efficiency.

An unexpected finding was the increase in SSI accidents when considering AV-pedestrian interactions (except for SD scenario). All SSI accidents were equal or more frequent. A possible explanation for this is that in the benchmark more PVs are present, but when there are less of them, they are further away from intersections, or approaching slower in the other scenarios, the AV is less likely to slow down when approaching an intersection. This can result in a reduction of safety for pedestrians as AVs pass the crossings with higher velocities (this phenomenon can also explain certain deviations in SSI accident frequency of AV-AV, AV-trailer, AV-car and AV-bike interactions).

It was observed in the SD scenario that there are equal or less recorded number of accidents for all SSIs and all entities (except for MTTC in the vehicle SSI assessment). Although it was initially not expected, it is only logical that the number of SSI accidents drop as the SSIs are all somehow related to speed and the average speed is lowered. The increase in number of accidents for the MTTC SSI is likely caused by the later braking of AV as they approach slower. When the AV does not decelerate, the value for MTTC is equal to the TTC. The threshold for MTTC is more than three times as high as TTC, causing the number of threshold violations to drastically increase.

When comparing the time loss of the AVs in the benchmark and the V2I, V2V, V2X and KC scenarios, it is clear that there is a considerable performance gain. These performance gains are statistically significant as confirmed by a t-test at the 0.05 significance level. Keeping a certain area around intersections clear could be a design requirement for new buildings as it improves the operational efficiency by 3%, but it is probably not economically viable to remove existing objects as the performance gain of adding communication devices is twice as big (6-8%). Interestingly, the V2I and V2V show only a 0.9% difference in performance gain, favoring V2I. But when considering installation and operational costs, only implementing V2V could be

considered as the AVs are already equipped with these sensors and only require an extra communication device. However, the static sensors of the V2I scenario are always present and could also collect valuable information of the traffic in zone. The highest performance gain has been achieved by the V2X scenario as it combines V2V and V2I. Other entities show no significant performance gain or reduction in the V2I, V2V, V2X and KC scenarios. The significant reduction in performance in the SD scenario for all entities is a logical consequence of adjusting the speed limit. It may be fairer to calculate the time loss fraction with the free flow data from the SD scenario network.

In short, lowering the allowed speed in the network results in a drastic reduction in occurrence of critical situations at the cost of efficiency for all road users. Adding any type of communication between AVs and/or infrastructure does not impact safety much, but drastically reduces the delay of the AVs, while other road users are not affected. Keeping a certain area around intersections clear of obstructions also does not impact safety, but results in a small reduction in delays of AVs.

8

Lessons learned

From this research some valuable lessons have been learned. This chapter is intended for policymakers in order to make well-informed decisions regarding the deployment of AVs. The eight major lessons learned in this this research are listed below:

1. The urban MFDs suggest that introducing a small fraction of AVs does not affect the network performance;
2. On the basis of time loss, introducing AVs does not affect the network performance;
3. Speed controller parameters mostly influence the level of safety (when using a perfect OAD model), not necessarily the network layout;
4. There is a trade-off between AV car-following time gap, average AV delay and safety slack;
5. Operational efficiency of AVs is greatly improved with various means of intervehicular communication, the delay of other vehicles is not majorly affected;
6. The safety performance is about equal when introducing communication devices;
7. Disallowing building close to intersections not majorly improves the operational efficiency or safety, but can be considered for new objects;
8. Lowering the speed limit is the best way to improve safety, but this may provoke other drivers to speed. Making the AV's OAD less effective as it expects other driver to adhere to the speed limit.

It is now known that introducing a small fraction of AVs will not result in any major changes in network performance or delay for conventional vehicles at the M4H. When designing a road network, minimizing the number of interactions between entities from different classes is the best practice from the safety perspective. Dividing traffic with exclusive lanes according to vehicle classes (bike lanes, sidewalks, etc.) is highly advised, but is already applied in the M4H network and in general in the Netherlands (Swov, 2020). Delaying entities because of conservative driving and simply lowering speed limits is not desired as it may provoke speeding, illegal overtaking, or other dangerous actions. Closely monitoring the vehicles and actively fining those who do not adhere to the rules could resolve these issues (Swov, 2016), but it is assumed that this will not benefit people's perception of AVs. It is therefore advised to adapt the roads in such a way that these actions are physically impossible.

In the particular case study of the M4H, introducing V2I is highly recommended. Aside from adding extra eyes to the AVs, valuable long-term data can be gathered on the behavior of entities in the zone under different conditions. Additionally, any accidents involving AVs are at high risk of going viral, damaging the reputation of the AV industry. The data can serve as evidence against the bad behavior of the AV. In the case an accident is actually caused by the

AV, this data can be used to analyze the critical event in great detail and to ultimately improve the driving model. Since everything in this world will soon be interconnected, it is believed that it is important for the municipality of Rotterdam to start experimenting with V2X technology on these AVs right away. This way, as V2X technology slowly gets available to human-driven vehicles, the necessary developments regarding the AVs are already in full swing. Keeping a certain area around intersections clear could be a design requirement for new buildings as it improves the operational efficiency of AVs by 3% and improves the visibility for all road users. But removing existing objects is not expected to be worth it from the AVs perspective, as the performance gain of adding any communication device is at least twice as big.

9

Conclusion

This study investigates the impact of introduction autonomous vehicles in an urban road network on traffic safety and operational efficiency, and how to mitigate the potential impact. The former Merwe- and Vierhavensgebied (M4H) in the Dutch city of Rotterdam was used as a use case. In 2035, this zone should be transformed to a vibrant new part of the city where new manufacturing industry, urban facilities, housing, and culture come together (*Toekomst in de Maak - Ruimtelijk Raamwerk Merwe-Vierhavensgebied Rotterdam*, 2019). It is believed that autonomous freight transport could play a part in the development of new manufacturing industry. The M4H case was used to answer the question: *How could a safe mixed traffic area for autonomous last-mile delivery of cargo be designed while taking operational efficiency into account?*

A framework was proposed in which virtual Autonomous Vehicles (AVs) can be injected in the microscopic traffic simulator SUMO, and be assessed in terms of safety with Surrogate Safety Indicators (SSIs) and operational efficiency. These AVs use an Occlusion Aware Driving (OAD) principle which takes the occluded sensorial view of AVs caused by objects into consideration. At the border of the AV's visibility range, Pseudo Vehicles (PVs) are added. By introducing these imaginary PVs, the AV should never be overwhelmed if an entity, which was previously behind an occlusion, appears. Although this driving principle is considered perfectly safe, it is also very conservative. To mitigate this, various countermeasures have been investigated by simulating the network under various scenarios.

The safety of a scenario was assessed by first identifying potential accidents using the Swedish TCT (STCT), PET, and DRAC with relaxed thresholds. Then, the potential accidents were subjected to tighter thresholds for the SSIs: STCT, TTC, TA, TIT, MTTC, CI, PET, PSD, DRAC, CrF, and PRI. The number of threshold violations for an SSI was divided by the number of interactions in that scenario. These fractions gave a good approximation of the amount of safety slack for the scenarios. Microscopic fundamental diagrams (MFDs) were used to assess the network operational efficiency. Furthermore, the average time loss compared to free-flowing traffic was used to determine the operational efficiency on a vehicular level.

A benchmark was made to verify the safety and operational efficiency assessment model. Several simulation scenarios were created, where the desired time gap of the AVs was varied. This variation also affects how fast AVs approach an intersection. The results showed strong evidence that there is a trade-off between safety and efficiency when varying the car-following parameters. It was proven that safety and efficiency analysis methods are sensitive enough to be influenced by driving parameters.

In the main experiment, a total of five additional scenarios with measures were investigated of which three were communication-based: V2I, V2V, and V2X. The other two were infrastructural based: reducing the maximum allowed speed for some lanes (SD) and keeping a certain area around intersections clear of obstructions (KC). The V2I, V2V, V2X, and KC scenarios showed similar levels of safety for trailers, cars, and bikes, but pedestrian safety slightly decreased. The operational efficiency based on time loss of AVs experienced a performance gain of 7.2%, 6.3%, 7.9%, and 3.0% for these scenarios, respectively. The time loss of the other entities was not affected. Due to the lowered allowed speed in certain lanes, the safety for all entities increased in the SD scenario, but at the cost of decreased operational efficiency of all entities.

Several limitations were identified during this study that could be the focus of future studies. On the simulations side, the relatively large time step of 1 second is good for approximating efficiency, but when assessing safety, it is suspected that lower discrete time steps would provide more accurate results. Aside from this limitation, the impact of emergency vehicles, the weather, lane changing, and overtaking is not investigated. Lane changing and overtaking is preventable in the real network, but emergency vehicles and weather changes are inevitable, and how to handle this should be thoroughly investigated before AV deployment. In this research, the safety is assessed using SSIs with braking as the evasive action, but in reality, swerving and accelerating also occur. By using the very conservative OAD principle, collisions cannot happen in the simulated environment as long as strange/random actions of actual drivers are not simulated. Therefore, a predicted crash rate cannot be given, and arbitrary values are used as thresholds for SSI collisions. This, however, still gives some indication of how much safety slack is in the network. As of now, no distinction was made between conflict location, conflict type, and vehicle types (except pedestrians) when assessing safety. To obtain a better understanding of the crash mechanisms, this could be considered.

To answer the main research question: the level of safety is mainly affected by the car-following time gap of the AVs as it adds extra time to execute potential evasive actions. However, there is a trade-off between safety and efficiency when varying this parameter. To mitigate the conservative behavior of the OAD principle, keeping a certain area around intersections clear could be a design requirement for new buildings as it improves the operational efficiency by 3%. But removing existing objects is not expected to be worth trying as the performance gain of adding any communication device is at least twice as big. Interestingly, the V2I and V2V show only a 0.9% difference in performance gain, favoring V2I. When considering costs, only implementing V2V could be considered as the AVs are already equipped with the correct sensors, but there have to be a certain number of AVs present in the zone to get the desired effect. A benefit of V2I is that they are always present and can collect valuable information about the traffic in the zone. The largest performance gain has been achieved by the V2X scenario as it combines V2V and V2I. Other entities show no significant performance gain or reduction in the V2I, V2V, V2X, and KC scenarios. In practice, lowering the speed limit is the absolute best way to avoid critical safety situations and reduce the severity of accidents, but it significantly impacts the delay of all entities, which may provoke dangerous behavior.

Bibliography

- Alhajyaseen, W. K. M. (2015). The Integration of Conflict Probability and Severity for the Safety Assessment of Intersections. *Arabian Journal for Science and Engineering*, 40(2), 421-430. doi:10.1007/s13369-014-1553-1
- Allen, B. L., Shin, B. T., & Cooper, P. J. (1978). ANALYSIS OF TRAFFIC CONFLICTS AND COLLISIONS. In *Transportation Research Record* (Vol. 667, pp. 67-74): Transportation Research Board.
- Almqvist, S., Hydén, C., & Risser, R. (1991). Use of speed limiters in cars for increased safety and a better environment. In *Transportation Research Record* (Vol. 1318): Transportation Research Board.
- Axelsson, E., & Wilson, T. (2016). *Microscopic simulation as an evaluation tool for the road safety of vulnerable road users*. (M.S. thesis), Linköping University, Norrköping, Sweden.
- Bagdadi, O. (2013). Estimation of the severity of safety critical events. *Accident Analysis & Prevention*, 50, 167-174. doi:<https://doi.org/10.1016/j.aap.2012.04.007>
- Baguley, C. (1984). The british traffic conflict technique. In *International Calibration Study of Traffic Conflict Techniques* (pp. 59-73): Springer.
- Barceló Bugeda, J., Dumont, A.-G., Montero Mercadé, L., Perarnau, J., & Torday, A. (2003). *Safety indicators for microsimulation-based assessments*. Paper presented at the Transportation Research Board 82nd Annual Meeting.
- Braam, L. (2018). *The Design of a Self Driving Container Chassis, The Electrical system* (2018.TEL.8258). Retrieved from Delft:
- Budan, G., Hayatleh, K., Morrey, D., Ball, P., & Shadbolt, P. (2018). An analysis of vehicle-to-infrastructure communications for non-signalised intersection control under mixed driving behaviour. *Analog Integrated Circuits and Signal Processing*, 95(3), 415-422. doi:10.1007/s10470-018-1152-2
- Bulla-Cruz, L. A., Laureshyn, A., & Lyons, L. (2020). Event-based road safety assessment: A novel approach towards risk microsimulation in roundabouts. *Measurement*, 165, 108192. doi:10.1016/j.measurement.2020.108192
- Cafiso, S., Garcia, A. G., Cavarra, R., & Rojas, M. R. (2011, Sep.). *Crosswalk safety evaluation using a pedestrian risk index as traffic conflict measure*. Paper presented at the Proceedings of the 3rd International Conference on Road safety and Simulation, Indianapolis, USA.
- Casares, M., Almagambetov, A., Velipasalar, S., & Ieee. (2012). *A Robust Algorithm for the Detection of Vehicle Turn Signals and Brake Lights*. Los Alamitos: Ieee Computer Soc.
- Ching-Yao, C. (2006, June.). *Defining Safety Performance Measures of Driver-Assistance Systems for Intersection Left-Turn Conflicts*. Paper presented at the 2006 IEEE Intelligent Vehicles Symposium.
- Cooper, P. J. (1984). Experience with traffic conflicts in Canada with emphasis on “post encroachment time” techniques. In *International calibration study of traffic conflict techniques* (pp. 75-96): Springer.
- Cunto, F. (2008). Assessing safety performance of transportation systems using microscopic simulation.
- Cunto, F. J. C., & Saccomanno, F. F. (2007). *Microlevel traffic simulation method for assessing crash potential at intersections*. Retrieved from
- Daganzo, C. F. (2005). A variational formulation of kinematic waves: basic theory and complex boundary conditions. *Transportation Research Part B: Methodological*, 39(2), 187-196. doi:<https://doi.org/10.1016/j.trb.2004.04.003>
- Daganzo, C. F., & Geroliminis, N. (2008). An analytical approximation for the macroscopic fundamental diagram of urban traffic. *Transportation Research Part B: Methodological*, 42(9), 771-781. doi:<https://doi.org/10.1016/j.trb.2008.06.008>

- Daganzo, C. F., & Lehe, L. J. (2016). Traffic flow on signalized streets. *Transportation Research Part B: Methodological*, 90, 56-69. doi:<https://doi.org/10.1016/j.trb.2016.03.010>
- Dickmanns, E. D. (2002). *The development of machine vision for road vehicles in the last decade*. Paper presented at the Intelligent Vehicle Symposium, 2002. IEEE.
- Dow, J. (2019, Oct. 23, 2019). Tesla updates Autopilot safety numbers; almost 9x safer than average driving. Retrieved 30-11-2020 from <https://electrek.co/2019/10/23/tesla-autopilot-safety-9x-safer-than-average-driving/>
- El-Basyouny, K., & Sayed, T. (2013). Safety performance functions using traffic conflicts. *Safety Science*, 51(1), 160-164. doi:<https://doi.org/10.1016/j.ssci.2012.04.015>
- Elvik, R. (1988). Some difficulties in defining populations of "entities" for estimating the expected number of accidents. *Accident Analysis & Prevention*, 20(4), 261-275. doi:10.1016/0001-4575(88)90054-1
- Erke, H., & Gstalter, H. (1985). *Verkehrskonflikttechnik : Handbuch f?r die Durchf?hrung und Auswertung von Erhebungen* (Vol. 52). Bremerhaven: Wirtschaftsverlag NW.
- Essa, M., & Sayed, T. (2015). Simulated Traffic Conflicts: Do They Accurately Represent Field-Measured Conflicts? *Transportation Research Record*, 2514(1), 48-57. doi:10.3141/2514-06
- Fancello, G., Carta, M., & Fadda, P. (2019). Road intersections ranking for road safety improvement: Comparative analysis of multi-criteria decision making methods. *Transport Policy*, 80, 188-196. doi:10.1016/j.tranpol.2018.04.007
- Galceran, E., Olson, E., & Eustice, R. M. (2015, 28 Sept.-2 Oct. 2015). *Augmented vehicle tracking under occlusions for decision-making in autonomous driving*. Paper presented at the 2015 IEEE/RSJ International Conference on Intelligent Robots and Systems (IROS).
- Gayah, V. V., & Dixit, V. V. (2013). Using Mobile Probe Data and the Macroscopic Fundamental Diagram to Estimate Network Densities: Tests Using Microsimulation. *Transportation Research Record*, 2390(1), 76-86. doi:10.3141/2390-09
- Geroliminis, N., & Boyacı, B. (2012). The effect of variability of urban systems characteristics in the network capacity. *Transportation Research Part B: Methodological*, 46(10), 1607-1623.
- Geroliminis, N., & Daganzo, C. F. (2008). Existence of urban-scale macroscopic fundamental diagrams: Some experimental findings. *Transportation Research Part B: Methodological*, 42(9), 759-770.
- Godfrey, J. W. (1969). The mechanism of a road network. *Traffic Engineering and Control*, 11(7), 323-327.
- Granath, E. (2020, 25-03-2020). 5 top autonomous vehicle companies to watch in 2020. Retrieved 30-11-2020-2020 from <https://www.intelligent-mobility-xperience.com/5-top-autonomous-vehicle-companies-to-watch-in-2020-a-958065/>
- Greenshields, B. d., Bibbins, J. r., Channing, W. s., & Miller, H. h. (1935). A study of traffic capacity. *Highway Research Board proceedings*, 1935, -.
- Guido, G., Astarita, V., Vitale, A., & Giofré, V. (2012). A new microsimulation model for the evaluation of traffic safety performances. *European Transport / Trasporti Europei*(51).
- Guido, G., Vitale, A., Astarita, V., & Giofre, V. P. (2019). Comparison Analysis between Real Accident Locations and Simulated Risk Areas in An Urban Road Network. *Safety*, 5(3). doi:10.3390/safety5030060
- Hansson, A. (1975). *STUDIES IN DRIVER BEHAVIOUR, WITH APPLICATIONS IN TRAFFIC DESIGN AND PLANNING: TWO EXAMPLES*. Retrieved from
- Hauer, E., & Hakkert, A. (1988). The extent and some implications of incomplete accident reporting. *Transportation Research Record*, 1185, 17.
- Helbing, D. (2009). Derivation of a fundamental diagram for urban traffic flow. *The European Physical Journal B*, 70(2), 229-241. doi:10.1140/epjb/e2009-00093-7
- Hennessy, D., & Wiesenthal, D. (1999). Traffic congestion, driver Stress, and driver aggression. *Aggressive Behavior*, 25, 409-423. doi:10.1002/(SICI)1098-2337(1999)25:6<409::AID-AB2>3.0.CO;2-0





- Hupfer, C. (1997). *Deceleration to safety time (DST)-a useful figure to evaluate traffic safety*. Paper presented at the ICTCT Conference Proceedings of Seminar.
- Hydén, C. (1996). Traffic conflicts technique: state-of-the-art. In *Traffic safety work with video processing* (Vol. 37, pp. 3-14).
- Johnsson, C., Lareshyn, A., & De Ceunynck, T. (2018). In search of surrogate safety indicators for vulnerable road users: a review of surrogate safety indicators. *Transport Reviews*, 38(6), 765-785. doi:10.1080/01441647.2018.1442888
- Kočárková, D. (2012). Traffic Conflict Techniques in Czech Republic. *Procedia - Social and Behavioral Sciences*, 53, 1029–1034. doi:10.1016/j.sbspro.2012.09.952
- KPMG. (2020). 2020 Autonomous Vehicles Readiness Index.
- Kraay, J., van der Horst, A., & Oppe, S. (2013). Manual conflict observation technique DOCTOR (Dutch Objective Conflict Technique for Operation and Research).
- Krauß, S. (1998). *Microscopic modeling of traffic flow: Investigation of collision free vehicle dynamics*. (dissertation), University of Cologne, Cologne.
- Kulmala, R. (1984). The Finnish traffic conflict technique. In *International Calibration Study of Traffic Conflict Techniques* (pp. 97-105): Springer.
- Lareshyn, A., Goede, M. d., Saunier, N., & Fyhri, A. (2017). Cross-comparison of three surrogate safety methods to diagnose cyclist safety problems at intersections in Norway. *Accident Analysis & Prevention*, 105, 11-20. doi:10.1016/j.aap.2016.04.035
- Lareshyn, A., & Varhelyi, A. (2018). *The Swedish traffic conflict technique: observer's manual*. Retrieved from https://lup.lub.lu.se/search/ws/files/51195704/TCT_Manual_2018.pdf
- Laval, J., & Castrillón, F. (2015). Stochastic Approximations for the Macroscopic Fundamental Diagram of Urban Networks. *Transportation Research Procedia*, 7, 615-630. doi:10.1016/j.trpro.2015.06.032
- Leclercq, L., Chiabaut, N., & Trinquier, B. (2014). Macroscopic Fundamental Diagrams: A cross-comparison of estimation methods. *Transportation Research Part B: Methodological*, 62, 1-12. doi:<https://doi.org/10.1016/j.trb.2014.01.007>
- Leclercq, L., & Geroliminis, N. (2013). Estimating MFDs in Simple Networks with Route Choice. *Procedia - Social and Behavioral Sciences*, 80, 99-118. doi:<https://doi.org/10.1016/j.sbspro.2013.05.008>
- Lee, M., Jo, K., & Sunwoo, M. (2017, 16-19 Oct. 2017). *Collision risk assessment for possible collision vehicle in occluded area based on precise map*. Paper presented at the 2017 IEEE 20th International Conference on Intelligent Transportation Systems (ITSC).
- Lekkerkerk, K. (2018). *Testing functionalities of a self-driving container chassis: an experimental setup for an intersection and accuracy analysis* (2018.TEL.8254). Retrieved from Delft:
- Li, S., Xiang, Q., Ma, Y., Gu, X., & Li, H. (2016). Crash Risk Prediction Modeling Based on the Traffic Conflict Technique and a Microscopic Simulation for Freeway Interchange Merging Areas. *International Journal of Environmental Research and Public Health*, 13, 1-14. doi:10.3390/ijerph13111157
- Lin, X., Zhang, J., Shang, J., Wang, Y., Yu, H., & Zhang, X. (2019, 27-30 Oct. 2019). *Decision Making through Occluded Intersections for Autonomous Driving*. Paper presented at the 2019 IEEE Intelligent Transportation Systems Conference (ITSC).
- Lu, Q., & Tettamanti, T. (2018). *Impacts of autonomous vehicles on the urban fundamental diagram*. Paper presented at the Road and Rail Infrastructure V, Zadar, Croatia. <https://master.grad.hr/cetra/ocs/index.php/cetra5/cetra2018/paper/viewFile/714/718>
- Lu, Q., Tettamanti, T., Hörcher, D., & Varga, I. (2019). The impact of autonomous vehicles on urban traffic network capacity: an experimental analysis by microscopic traffic simulation. *Transportation Letters*, 12(8), 540-549. doi:10.1080/19427867.2019.1662561
- Mahmud, S. M. S., Ferreira, L., Hoque, M. S., & Tavassoli, A. (2017). Application of proximal surrogate indicators for safety evaluation: A review of recent developments and research needs. *latss Research*, 41(4), 153-163. doi:10.1016/j.iatssr.2017.02.001


- Minderhoud, M. M., & Bovy, P. H. L. (2001). Extended time-to-collision measures for road traffic safety assessment. *Accident Analysis & Prevention*, 33(1), 89-97. doi:[https://doi.org/10.1016/S0001-4575\(00\)00019-1](https://doi.org/10.1016/S0001-4575(00)00019-1)
- Muhlrad, N., & Dupre, G. (1984). The French conflict technique. In *International Calibration Study of Traffic Conflict Techniques* (pp. 121-132): Springer.
- Okamura, M., Fukuda, A., Morita, H., Suzuki, H., & Nakazawa, M. (2011). Impact evaluation of a driving support system on traffic flow by microscopic traffic simulation. *Advances in Transportation Studies*(Special Issue 2011).
- Orzechowski, P. F., Meyer, A., & Lauer, M. (2018, 4-7 Nov. 2018). *Tackling Occlusions & Limited Sensor Range with Set-based Safety Verification*. Paper presented at the 2018 21st International Conference on Intelligent Transportation Systems (ITSC).
- Ozbay, K., Yang, H., Bartin, B., & Mudigonda, S. (2008). Derivation and Validation of New Simulation-Based Surrogate Safety Measure. *Transportation Research Record*, 2083(1), 105-113. doi:10.3141/2083-12
- Parker Jr, M., & Zegeer, C. V. (1989). *Traffic conflict techniques for safety and operations: Observers manual*. Retrieved from
- Pauwels, A. (2020). Suitable Zone Selection for Testing Autonomous Last-Mile Container Cargo Delivery in the Municipality of Rotterdam.
- Payne, H. J. (1979). FREFLO: A macroscopic simulation model of freeway traffic. *Transportation Research Record*(722).
- Risser, R., Tamme, W., STEINBAUER, J., & KABA, A. (1991). Handbuch zur Erhebung von Verkehrskonflikten mit Anleitungen zur Beobachterschulung. *KLEINE FACHBUCHREIHE DES KURATORIUMS FUER VERKEHRSSICHERHEIT (KFV)*(28).
- Sathya, R., Geetha, M. K., & Aboorvapiya, P. (2015). Vehicle Brake and Indicator Detection for Autonomous Vehicles. In J. H. Abawajy, S. Mukherjea, S. M. Thampi, & A. RuizMartinez (Eds.), *Security in Computing and Communications* (Vol. 536, pp. 392-401). Berlin: Springer-Verlag Berlin.
- Saunier, N., & Sayed, T. (2007). Automated analysis of road safety with video data. *Transportation Research Record*(2019), 57-64. doi:10.3141/2019-08
- Shelby, S. G. (2011). *Delta-V as a measure of traffic conflict severity*. Paper presented at the 3rd International Conference on Road Safety and Simulati. September.
- Shoufeng, L., Jie, W., van Zuylen, H., & Ximin, L. (2013). *Deriving the Macroscopic Fundamental Diagram for an urban area using counted flows and taxi GPS*. Paper presented at the 16th international IEEE conference on Intelligent Transportation Systems (ITSC 2013).
- Siegel, J., & Coeymans, J. E. (2005). An Integrated Framework for Traffic Analysis Combining Macroscopic and Microscopic Models. *Transportation Planning and Technology*, 28(2), 135-148. doi:10.1080/03081060500053533
- Smeed, R. J. (1968). Traffic studies and urban congestion. *Journal of Transport Economics and Policy*, 33-70.
- SUMO - Definition of Vehicles, Vehicle Types, and Routes. (2020). Retrieved 28-1-2010 from https://sumo.dlr.de/docs/Definition_of_Vehicles,_Vehicle_Types,_and_Routes.html#ar-following_model_parameters
- SUMO - Vehicle Type Parameter Defaults. (2019). Retrieved 28-1-2010 from https://sumo.dlr.de/docs/Vehicle_Type_Parameter_Defaults.html
- Svensson, Å. (1992). Vidareutveckling och validering av den svenska konflikttekniken. *Lund, Sweden: Dept of Technology and Society. LTH, Lund University*.
- Svensson, Å., & Hydén, C. (2006). Estimating the severity of safety related behaviour. *Accident Analysis & Prevention*, 38(2), 379-385. doi:10.1016/j.aap.2005.10.009
- Swov. (2016). *Snelheid en snelheidsmanagement*. Retrieved from Den Haag:
- Swov. (2020). *Infrastructuur voor voetgangers en fietsers*. Retrieved from Den Haag:
- Tafidis, P., Pirdavani, A., Brijs, T., & Farah, H. (2019). Can Automated Vehicles Improve Cyclist Safety in Urban Areas? *Safety*, 5(3), 1-13. doi:10.3390/safety5030057

- Tarko, A., Davis, G., Saunier, N., & Sayed, T. (2009). *European Transport / Trasporti Europei*. Retrieved from
- Toekomst in de Maak - Ruimtelijk Raamwerk Merwe-Vierhavensgebied Rotterdam. (2019). Retrieved from <https://m4hrotterdam.nl/wp-content/uploads/2019/07/DLA-M4H-17028-Boekwerk-190627-LQ.pdf>
- Topham, G. (2020). Self-driving cars could be allowed on UK motorways next year. *The Guardian*. Retrieved from <https://www.theguardian.com/technology/2020/aug/18/self-driving-cars-allowed-motorways-industry-risk>
- Uno, N., Iida, Y., Itsubo, S., & Yasuhara, S. (2002). *A microscopic analysis of traffic conflict caused by lane-changing vehicle at weaving section*. Paper presented at the Proceedings of the 13th Mini-EURO Conference-Handling Uncertainty in the Analysis of Traffic and Transportation Systems, Bari, Italy.
- Urmson, C., Anhalt, J., Bagnell, D., Baker, C., Bittner, R., Clark, M. N., . . . Ferguson, D. (2009). Autonomous Driving in Urban Environments: Boss and the Urban Challenge. In M. Buehler, K. Iagnemma, & S. Singh (Eds.), *The DARPA Urban Challenge: Autonomous Vehicles in City Traffic* (pp. 1-59). Berlin, Heidelberg: Springer Berlin Heidelberg.
- Várhelyi, A. (1998). Drivers' speed behaviour at a zebra crossing: a case study. *Accident Analysis & Prevention*, 30(6), 731-743. doi:[https://doi.org/10.1016/S0001-4575\(98\)00026-8](https://doi.org/10.1016/S0001-4575(98)00026-8)
- Virdi, N., Grzybowska, H., Waller, S. T., & Dixit, V. (2019). A safety assessment of mixed fleets with Connected and Autonomous Vehicles using the Surrogate Safety Assessment Module. *Accident Analysis and Prevention*, 131, 95-111. doi:10.1016/j.aap.2019.06.001
- Wang, Q., Li, L., Hou, D. Z., Li, Z. H., & Hu, J. M. (2020). Simulation study on the effect of automated driving in a road network environment. *Iet Intelligent Transport Systems*, 14(4), 228-232. doi:10.1049/iet-its.2019.0395
- Yu, M., Vasudevan, R., & Johnson-Roberson, M. (2019). Occlusion-Aware Risk Assessment for Autonomous Driving in Urban Environments. *Ieee Robotics and Automation Letters*, 4(2), 2235-2241. doi:10.1109/LRA.2019.2900453
- Yurtsever, E., Lambert, J., Carballo, A., & Takeda, K. (2020). A Survey of Autonomous Driving: Common Practices and Emerging Technologies. *Ieee Access*, 8, 58443-58469. doi:10.1109/access.2020.2983149
- Zapp, A. (1988). *Automatische Straßenfahrzeugführung durch Rechnersehen*: na.
- Zhang, L. L., Yuan, Z. Q., Yang, L., & Liu, Z. Y. (2020). Recent developments in traffic flow modeling using macroscopic fundamental diagram. *Transport Reviews*, 40(4), 529-550. doi:10.1080/01441647.2020.1743918

Appendix A Vehicle parameters

Table 16 Default vehicle parameters
(Braam, 2018; Lekkerkerk, 2018; "SUMO - Vehicle Type Parameter Defaults," 2019).

vClass	Picture	Length	a_{\max}	b	b_e	v_{\max}
		width				
pedestrian		0.22 m 0.48 m	1.5 m/s ²	2 m/s ²	5 m/s ²	5.4 km/h
bike		1.6 m 0.65 m	1.2 m/s ²	3 m/s ²	7 m/s ²	20 km/h
car		4.3 m 1.8 m	2.9 m/s ²	7.5 m/s ²	9 m/s ²	180 km/h
trailer		16.5 m 2.55 m	1.1 m/s ²	4 m/s ²	7 m/s ²	130 km/h

vClass	Picture	Length width	a_{max}	b	b_e	v_{max}
AV		16.5 m 2.55 m	1.1 m/s ²	4 m/s ²	7 m/s ²	50 km/h (in zone)
a_{max} = maximum acceleration b_{decel} = deceleration			v_{max} = maximum speed b_e = emergency deceleration			

Appendix B Additional MFDs (time gap)

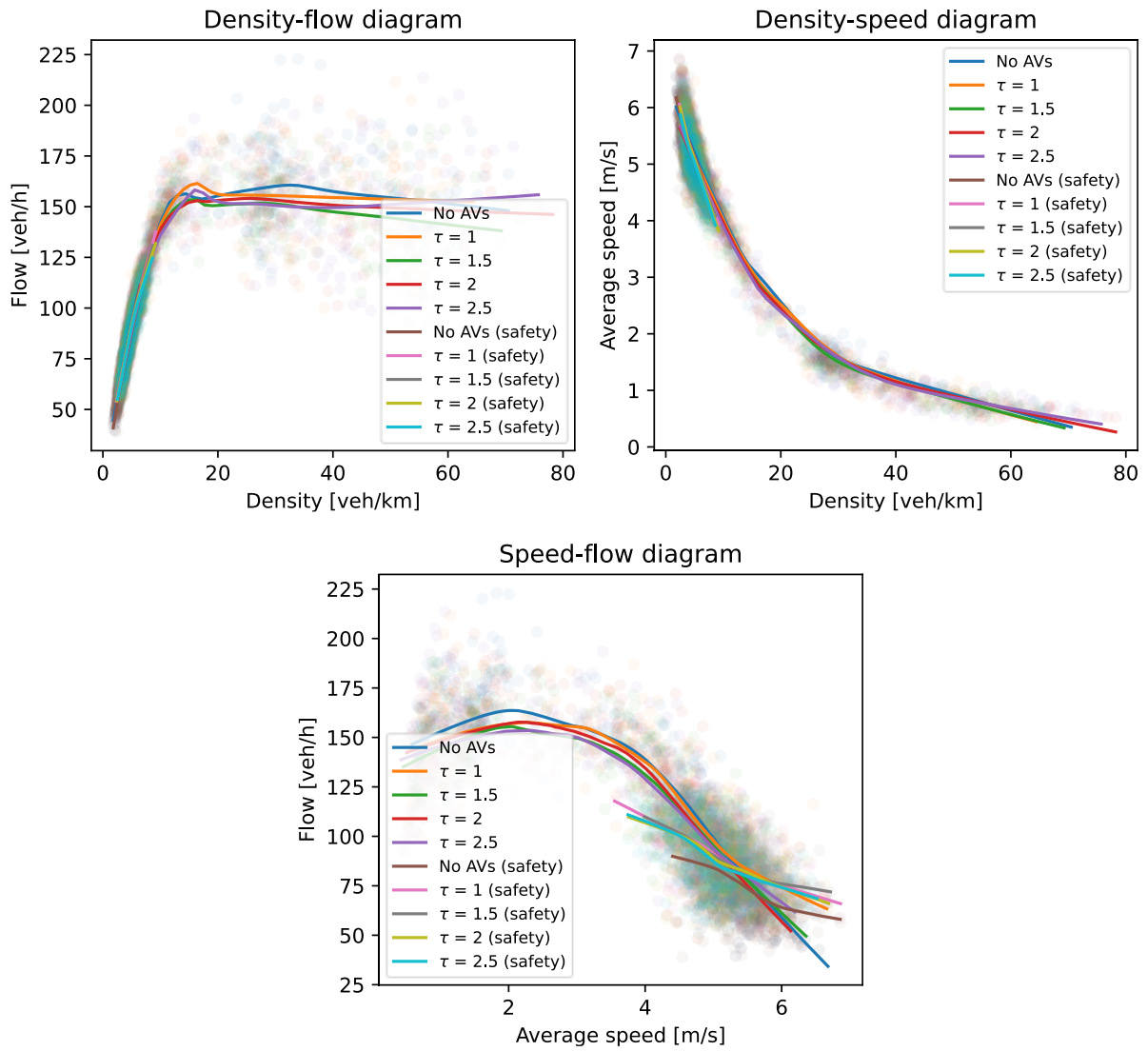


Figure 24 MFD of the benchmark scenarios with the results of the safety assessment indicated with (safety).

Appendix C Additional MFDs (measures)

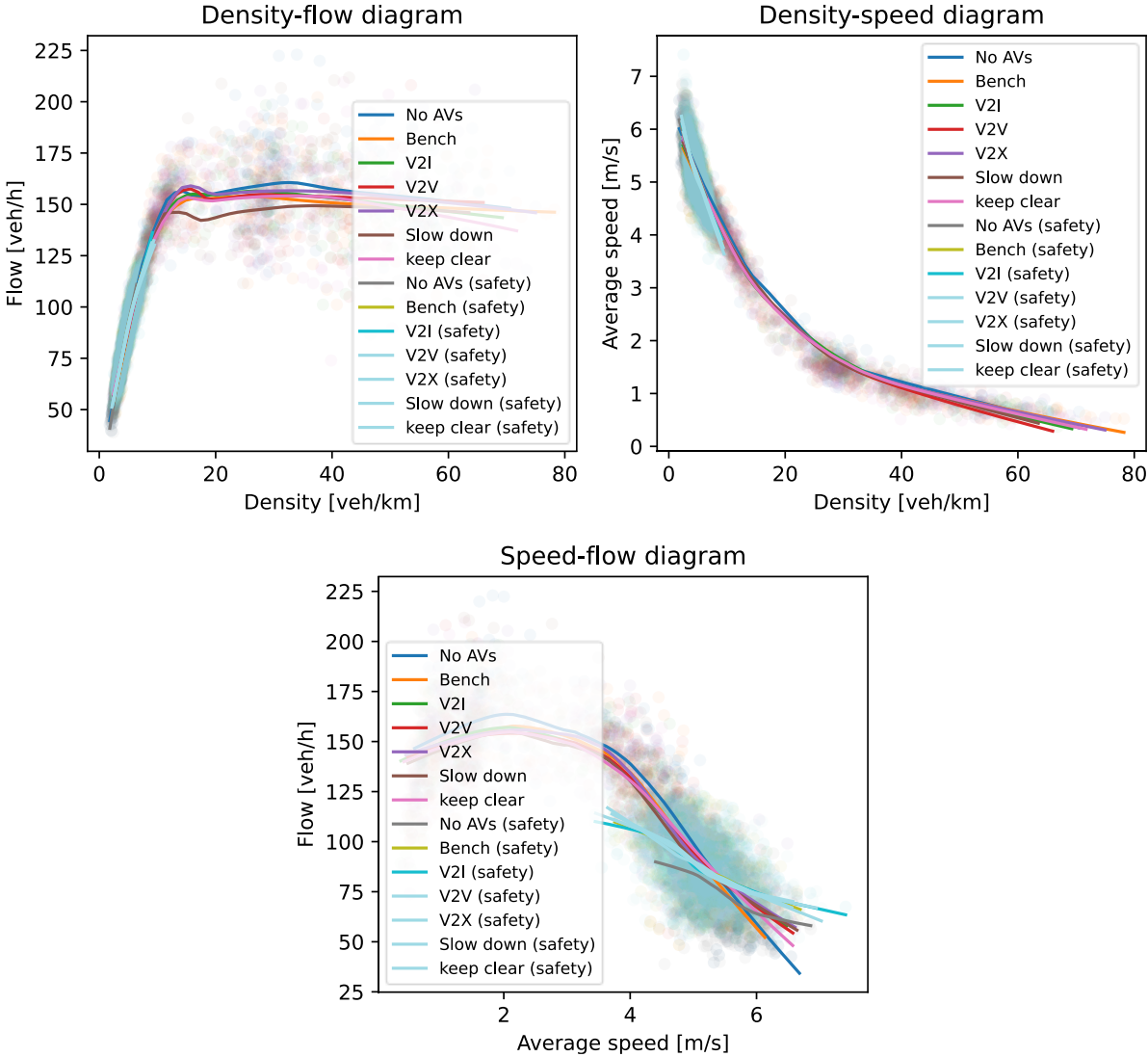


Figure 25 MFD of the main experiment scenarios with the results of the safety assessment indicated with (safety).